

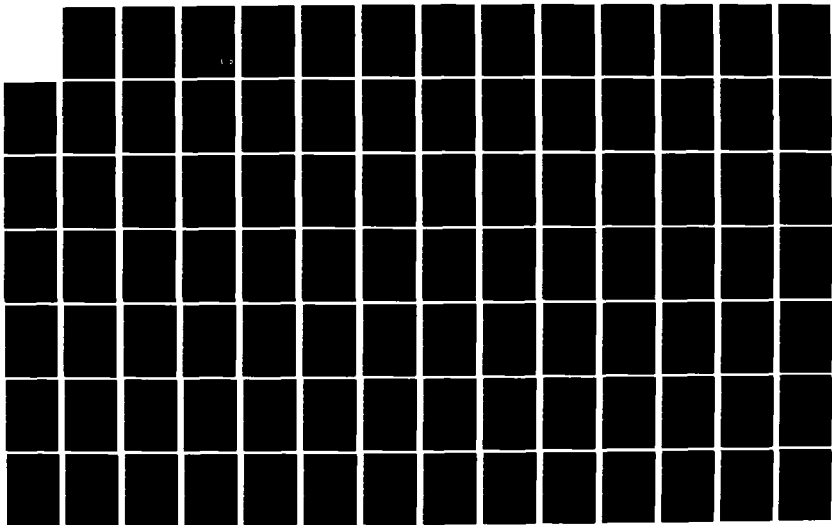
AD-A127 514

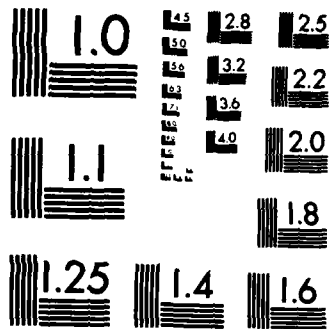
THE NET EFFECT OF MANY GRAVITATIONAL FIELDS ON THE  
INTENSITY OF CELESTIAL (U) AIR FORCE INST OF TECH  
WRIGHT-PATTERSON AFB OH SCHOOL OF ENGI... G E CIPPERLY  
DEC 82 AFIT/GEP/PH/82D-4 F/G 3/2

1/2

UNCLASSIFIED

NL





MICROCOPY RESOLUTION TEST CHART  
NATIONAL BUREAU OF STANDARDS-1963-A

A127514



THE NET EFFECT OF MANY GRAVITATIONAL FIELDS  
ON THE INTENSITY OF CELESTIAL LIGHT SOURCES

THESIS

AFIT/GEP/PH/82D-4

George E. Cipperly  
Captain USAF

THIS IS A COPY

This document has been approved  
for public release and sale  
without restriction.

DEPARTMENT OF THE AIR FORCE  
AIR UNIVERSITY (ATC)  
**AIR FORCE INSTITUTE OF TECHNOLOGY**

Wright-Patterson Air Force Base, Ohio

83 04 28 108

**DTIC**  
**ELECTE**  
MAY 02 1983  
**S**  
**E**

①

THE NET EFFECT OF MANY GRAVITATIONAL FIELDS  
ON THE INTENSITY OF CELESTIAL LIGHT SOURCES

THESIS

AFIT/GEP/PH/82D-4

George E. Cipperly  
Captain USAF

DTIC  
ELECTE  
MAY 02 1983  
S E D

Approved for public release; distribution unlimited.

THE NET EFFECT OF MANY GRAVITATIONAL FIELDS  
ON THE INTENSITY OF CELESTIAL  
LIGHT SOURCES

THESIS

Presented to the Faculty of the School of Engineering  
of the Air Force Institute of Technology  
Air University  
in Partial Fulfillment of the  
Requirements for the Degree of  
Master of Science

by

George E./Cipperly

Captain USAF

Graduate Engineering Physics

December 1982

Accession For	
NTIS GRA&I	<input checked="" type="checkbox"/>
DTIC TAB	<input type="checkbox"/>
Unannounced	<input type="checkbox"/>
Justification	
By _____	
Distribution/	
Availability Codes	
Dist	Avail and/or Special
A	



Approved for public release; distribution unlimited.

## Preface

Although this study treats the propagation of light in the vacuum of space, the problem was suggested by the similarity of random gravitational fields with the random density variations in the atmosphere, and is thus closely related to propagation of light in an inhomogeneous medium, a topic of contemporary concern to the military with regards to both sensor performance and laser propagation. The problem was posed by Dr. Richard Cook, whom I thank both for suggesting a thesis topic in line with my interests, and for his great help as my thesis advisor. His insight into the physical processes, and his assistance in mathematical troubleshooting were invaluable.

George E. Cipperly

Contents

	Page
Preface . . . . .	ii
List of Figures . . . . .	v
List of Symbols and Values . . . . .	vi
Abstract . . . . .	ix
I. Introduction . . . . .	1
Terminology . . . . .	1
Background . . . . .	1
Problem Statement . . . . .	5
Assumptions and Approximations . . . . .	5
General Approach . . . . .	7
II. Intensity Distance Measurements . . . . .	9
Scenarios for Intensity Distance Measurement . . . . .	9
Accuracy of Intensity Distance Measurements . . . . .	10
Worst Case Scenarios . . . . .	13
Pertinent Astrophysical Quantities . . . . .	14
III. Gravitational Index of Refraction . . . . .	17
IV. Effect of a Single Deflecting Mass on Intensity . . . . .	20
Paraxial Approach to Light Propagation . . . . .	20
Solution of the Paraxial Equations . . . . .	26
V. Approximation of the Single Mass Intensity Expression, and Its Validity . . . . .	31
Approximation for $r^2 \gg 4MGz/c^2$ . . . . .	31
Applicability of the Condition $r^2 \gg 4MGz/c^2$ . . . . .	33
Observation of Distant Sources through the Milky Way . . . . .	36
Observation of Stars Through Other Galaxies . . . . .	40
Observation of Remote Galaxies Through the Universal Distribution of Galaxies . . . . .	41
VI. Statistical Analysis . . . . .	44
Total Intensity Change Due to Many Deflectors . . . . .	44
Mean Gravitational Intensity Change . . . . .	45

	Page
Variance in the Distribution of Intensities . . . . .	53
Numerical Evaluation of Intensity Effects . . . . .	58
Discussion of Results . . . . .	59
VII. Conclusion . . . . .	65
Bibliography . . . . .	67
Appendix A: Summary of Pertinent Calculations from General Relativity . . . . .	69
Appendix B: 4-Space Calculation of the Deflection of Light Rays . . . . .	85
Appendix C: Justification of Approximations . . . . .	93
VITA . . . . .	110



List of Figures

Figure		Page
1	Portrayal of the "Gravitational Lens" Effect with Real and Virtual "Images" . . . . .	3
2	Depiction of the Single Mass Ray Deflection Problem . . . . .	22
3	Cross Section of the Paraboloidal Region Restricted to Deflecting Masses Obeying Condition (5-4) for a Given Observer . . . . .	35
4	Comparison of the Region of Unresolved Stellar Deflecting Masses with the Region of Masses Causing More than a 2% Intensity Change . . . . .	39
5	Geometry of the Limited Region Considered to Contain Deflecting Masses . . . . .	46
6	Volume Within Which Extended Bodies Would Physically Mask Extended Sources . . . . .	95
7	Rays Deflected by a Point Mass and Their Asymptotes . . . . .	104

## List of Symbols and Values

### Constants

$c$	= speed of light	= $3 \times 10^{10}$ cm/sec or $10^{-8}$ pc/sec
$G$	= universal gravitational constant	= $6.67 \times 10^{-8}$ cm <sup>3</sup> /g-sec <sup>2</sup>
$H_0$	= Hubble's constant	= 75km/sec/Mpc

### Units

1"arc	= one second of arc	= $4.85 \times 10^{-6}$ radians
A.U.	= Astronomical Unit (radius of earth orbit)	= $1.5 \times 10^{13}$ cm
Parsec (pc)	= distance at which 1 A.U. would subtend 1" arc	= $3 \times 10^{18}$ cm or $2 \times 10^5$ A.U.

### Symbols and Values

$z$	= coordinate along line of sight to a source	
$\theta$	= cylindrical angular coordinate	
$\rho$	= radial distance in spherical coordinates	} Note: Used differently in Appendices A & B
$r$	= radial distance in cylindrical coordinates	
$r_0(r,z)$	= value of $r$ at $z = 0$ for a ray passing through $(r,z)$	
$r_p(z)$	= radius of a certain paraboloid at height $z$	= $\sqrt{10Fz}$
$r_m$	= maximum value of $r_p$ in the region of interest	
$R$	= Minimum distance to edge of deflector field from line of sight to a source	
$R_\odot, R_s$	= radius of the sun or typical star	= $7 \times 10^{10}$ cm
$R_g$	= radius of galactic disk	= $1.25 \times 10^4$ pc

$R_u$	= radius of observable universe	= $4 \times 10^9$ pc
$\Delta z$	= that part of the distance to a source lying within a distribution of deflecting masses	
L.D.	= lateral displacement at the observer, of a deflected light ray	
V	= volume	
$V_p$	= volume of a truncated paraboloid ( $V_{pg}$ and $V_{pu}$ designate galactic or universal extent)	
p	= probable number of deflectors within some volume	
N	= total number of deflecting bodies in region of concern	
$\sigma$	= population density of deflecting masses or mass density of a body	
$\sigma_s$	= mean density of stars along galactic diameter	= $0.1 \text{ pc}^{-3}$
$\sigma_g$	= mean density of galaxies in the universe	= $3 \times 10^{-18} \text{ pc}^{-3}$
M	= mass	
$M_\odot$	= mass of the sun	= $2 \times 10^{33}$ g
$M_s$	= mass of typical star	= $3 \times 10^{33}$ g
$M_g$	= mass of typical galaxy	= $10^{44}$ g
F	= $4MG/c^2$	
$F_s$	= stellar F	= $3 \times 10^{-13}$ pc or $6 \times 10^{-8}$ A.U.
$F_g$	= galactic F	= $10^{-2}$ pc
$\Gamma$	= deflection of a light ray (tangent of angle or small angle itself)	
$\phi$	= classical gravitational potential	= $-MG/\rho$ for point mass
$\lambda$	= wavelength	

$k$	= propagation constant	= $2\pi/\lambda$
$n$	= index of refraction	
$\tilde{n}$	= $n-1$	
$\phi$	= phase of electromagnetic wave	
$E, P \& U$	= complex valued electromagnetic field strengths	
$A$	= real valued electromagnetic field amplitude	
$P_o$	= total power passing a specified area	
$I$	= intensity, electromagnetic power per unit area	= $U*U = A^2$
$I_o$	= uniform intensity of incident plane wave prior to perturbation	
$I_T$	= total intensity in the combined field of many deflectors	
$\langle I_T \rangle$	= mean intensity at a given distance in a random field of deflectors	
$D_I$	= mean deviation in intensities	
$D_{2I}$	= root mean square deviation in intensities	
$w$	= parameter indicative of the level of accuracy associated with a particular scenario	

## Abstract

→ This thesis investigates the lens-like action of the gravitational fields of celestial bodies, which can alter the apparent intensity of more distant sources. Previous work in this area has shown that the chance of an individual body being sufficiently well aligned with a source to cause a very large gravitational intensity change is small. The issue addressed in this study is the possibility of there being a significant total change in the intensity of a source due to the combined effects of the gravitational fields of all celestial bodies, and in particular, the potential impact on intensity distance measurements, that is, determination of the distances of celestial light sources by means of intensity comparisons.

It is first shown that the problem can be treated in flat space by associating an appropriate index of refraction with gravitational fields. A wave approach is taken in deriving the total deflection of a ray by the field of a single point mass. A statistical analysis is then performed to determine the expression for the mean total change in the intensity of celestial light sources due to the combined fields of all intervening bodies. ← This expression is evaluated using idealized populations for the cases of deflection by stars in the Milky Way and in other galaxies, as well as deflection by whole galaxies. Furthermore, due to the rapid drop in the effects of deflecting masses with their distance from the line of sight to a source, it is seen that any large intensity change would most likely be due to the individual effect of a

single closely aligned mass. The probability of such large individual effects, in agreement with previous work, is in most cases negligibly small. In view of the level of accuracy associated with intensity distance determinations, the mean net effect is also negligibly small. For galactic sources, however, the typical changes may be large enough to be observable if any rapid enough time variations occur.

THE NET EFFECT OF MANY GRAVITATIONAL FIELDS  
ON THE INTENSITY OF CELESTIAL  
LIGHT SOURCES

I. Introduction

Terminology

In this report, the intensity of a celestial object refers to the total power from it incident on a unit cross sectional area, that is, its associated irradiance. Also, the word "significant" is accorded its standard English definition rather than its special meaning in the field of statistics.

Throughout this study, the discussion freely varies between ray and wave terminology, as best suits particular arguments. Since rays are uniquely defined by the normals to the wave fronts, and are thus described by the full gradient of the phase, the entire analysis could theoretically be accomplished using either concept.

Background

In the early 1900s, Einstein developed the general theory of relativity and showed that one consequence was the bending of light rays in a gravitational field in a vacuum. Such ray bending was first verified by Eddington in 1919 when he measured the deflection of star light passing near the sun.

For a source and a deflecting mass nearly in line with a distant observer, this ray bending can produce a "gravitational lens" effect.

The exaggerated depiction in Figure 1 of a ray bundle under the action of a deflecting mass portrays the sort of lens action referred to in the simplest case, that of a point source and a spherically symmetric mass. (A similar bundle following a path around the opposite side of the deflector is not shown.) The lens is astigmatic in a rather unusual way. Ray path variation in the radial direction gives a diverging lens effect, while path variation in the tangential direction produces converging lens behavior, the result being that both a real and a virtual image are produced. Furthermore, the lens must be considered severely aberrated in that for a point source, both images are cast onto lines rather than points. The virtual image line is actually a ring segment and would be a complete ring, circling the deflecting mass, for a perfect alignment of the source, deflector and observer. As the alignment degrades, the image breaks into two decreasing segments of the ring, centered at the points where it intersects the plane determined by the source, deflector, and observer. The image formed by those rays taking the longer path around the deflector becomes dimmer and closer to the line of sight to the deflector, making it more and more difficult to observe. (In the case of extended, and perhaps irregular, sources and deflectors, more complex results can occur, including the production of more than two images.)

In the case of stars, Einstein showed that while multiple imaging was physically possible, the number of stars in our galaxy is such that the probability of two of them being sufficiently well aligned with the earth for the effect to be observed is negligibly small (Ref 1). Zwicky, in 1937, showed that the chances are much greater of observing



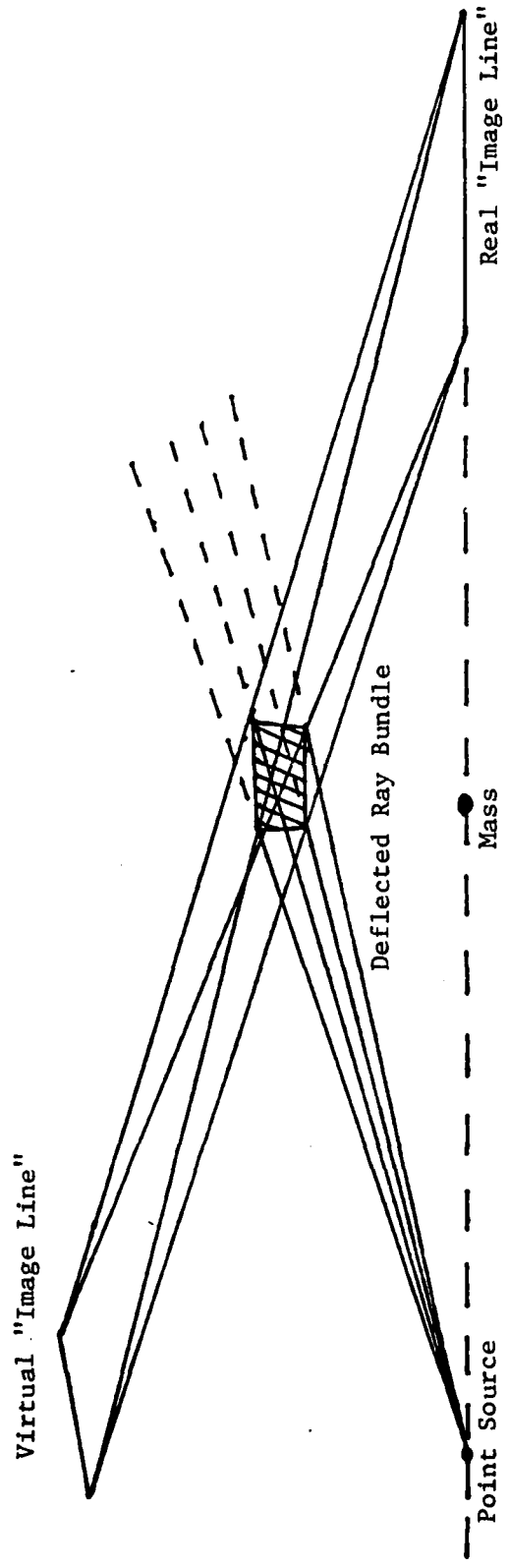


Figure 1. Portrayal of the "Gravitational Lens" Effect with Real and Virtual "Images"

such an effect among distant galaxies (Refs 2 and 3). Later, others considered the possible involvement of quasars in gravitational imaging (Refs 4 and 5). Over 40 years passed, however, before the effect was actually observed.

Finally, in the period from 1979 to 1981, observations of the double quasar 0957+561A,B suggested that it might be the double image of a single quasar produced by the gravitational field of an intervening elliptical galaxy (Refs 6 through 10). The question of whether this was indeed the correct explanation was ultimately resolved when Young, et al. (Ref 11) developed a theory of extended deflectors consisting of discrete masses, satisfactorily explaining all the known details of 0957+561A,B. This double quasar, then, provides additional evidence that the gravitational bending of light rays is a real phenomenon.

Another result of ray bending, less striking perhaps than multiple imaging, is a change in the intensity of distant objects due to the gravitational fields of intervening masses not necessarily so well aligned. The net effect of the combined gravitational fields of all celestial objects is to make the vacuum of space behave like an inhomogeneous medium with regard to the propagation of light. As a result, intensities can be expected to deviate randomly from those calculated solely from the inverse square distance relation. And, in fact, Cook, using general principles of light propagation in an inhomogeneous medium, showed that the statistical variance in the intensity of stars in our galaxy is of the order of the mean intensity itself (Ref 12). This suggests serious implications for the common

method of determining the distance to a star by comparing its intensity with that of similar stars at distances short enough to be measured by other means.

#### Problem Statement

The problem addressed in this study is to investigate the magnitude and statistical nature of changes in the intensity of celestial light sources due to the combined gravitational fields of all deflecting masses. Typical star and galaxy populations are used to determine whether possible large intensity changes are frequent enough to be taken into consideration when making intensity distance determinations, or whether the large variance is essentially due only to the sizeable contributions from very close alignments, in which case the effect can be ignored except in cases where a deflector appears so closely aligned with a source that a large individual effect is suggested. Such gravitational intensity changes could be troublesome since, unlike multiple imaging, it would be difficult to prove that they are occurring unless motion of the bodies involved produces a rapid enough time variation. (Previous work in this area has generally been directed toward determining the probability of finding individual deflecting masses sufficiently well aligned to produce multiple imaging or very large intensity variations.)

#### Assumptions and Approximations

The principal assumptions made in this study involve the values accepted for various astrophysical quantities. These quantities are known to varying levels of accuracy, and in many cases only a reasonable

estimate can be made. Furthermore, in order to accomplish calculations it is assumed that valid results can be obtained using only average values and idealized distributions. The use of such idealizations in worst case scenarios is in keeping with the objective of the study which is to place a bound on the mean magnitude of gravitational effects. Those actual values accepted for various quantities are described in Chapter II.

Another assumption is that secondary gravitational images would be identified as distinct sources, and so their intensities would be measured separately. Therefore, only the intensity contribution of primary images is considered.

Finally, it is assumed that several approximations made to facilitate calculations are valid. These approximations are, however, justified and discussed in Appendix C. The justifications incorporate the astrophysical quantities given in Chapter II, as well as some of the intermediate results of this study. The approximations are:

1. All sources are treated as point sources.
2. Gravitationally deflecting bodies are treated as point masses.
3. Sources are considered sufficiently distant that their actual spherical wave output can be adequately treated as plane waves in the neighborhoods of deflectors and the observer.
4. Monochromatic radiation in the geometrical optics limit is considered in the analysis.
5. Gravitational field effects are compressed into a thin phase screen located in the plane containing the deflecting mass and

orthogonal to the propagation direction. As a result, the actual hyperbolic ray trajectories around individual deflectors are approximated by their asymptotes.

6. The entire analysis is based on the weak field solution to the gravitational field equations shown in Appendix A. Its validity is therefore limited to weak field regions, that is, those characterized by the condition

$$\rho \gg \frac{4MG}{c^2} \equiv F \quad (1-1)$$

where  $\rho$  is the distance from the center of the deflecting mass,  $M$  is the total mass,  $G$  is the universal gravitational constant,  $c$  is the speed of light, and the quantity  $F$  has been defined for convenience.

7. In the course of the analysis several paraxial approximations are made. These approximations are based generally on the assumption that ray deflections in weak gravitational fields are so small that in some places the deflected rays can adequately be represented by undeflected rays. In wave terminology, the assumption is that incident waves are perturbed so slightly by weak fields that the resulting waves can be considered to propagate in the original direction, but with perturbed phase fronts.

#### General Approach

Following a review of pertinent astronomical facts and figures, the calculations in this report begin with the generally known weak field solution to the gravitational field equations. (A summary of the pertinent, basic results of general relativity, including the solution

to the weak field equations, is found in Appendices A and B.) The first step is to show that the behavior of light in the presence of gravity can be accounted for in a flat, 3-space analysis by associating an appropriate index of refraction with gravitational fields. Using this index of refraction and a paraxial approach to light propagation, equations are derived for the phase and intensity of electromagnetic waves passing a point mass. These equations are solved using geometrical arguments to get an expression for the intensity of an initially uniform plane wave after it has passed a single point mass.

A distribution of deflecting masses is then examined and expressions for the mean intensity change and its variance are derived. Actual populations of celestial objects are used both to justify simplifications and to numerically evaluate the final statistical results in some limiting cases.

## II. Intensity Distance Measurements

Since the objective of this study is to determine the impact of gravitational intensity variations on distance measurements, the various scenarios in which such intensity distance measurements are made and the associated levels of accuracy are first reviewed. Also, the actual deflecting mass populations in these scenarios must be established so that they can be used in determining the validity of certain approximations, as well as in numerically evaluating the final statistical results.

### Scenarios for Intensity Distance Measurement

Out to about 30 pc, the primary distance measurement technique is direct measurement of parallax, or the angle of apparent motion of the measured object against the "fixed" more distant background as the earth moves in its orbit. A less accurate, statistical analysis of the motions of the stars in a cluster can be used to determine distances out to over 100 pc (Ref 13). For distances greater than this, intensity comparison becomes the primary distance measurement technique. (intensity measurements are important at closer ranges as well, however, for determining the scale of the intensity yardstick.)

The well defined relation between spectral type and absolute magnitude for stars on the main sequence of the Hertzsprung-Russell diagram enables intensity comparison to be used in determining the distance of main sequence stars in our galaxy. The fixed relation between magnitude and period for several types of variable stars allows fairly

accurate intensity distance determinations for galaxies out to about  $4 \times 10^6$  pc in which such variables can be resolved. The less well defined typical intensity of globular clusters or brightest stars in a galaxy stretches this limit out to their maximum distance of resolvability of about  $10^8$  pc, which reaches the nearest, or Virgo, cluster of galaxies. Further out still, the typical absolute magnitude of the brightest elliptical galaxy in a cluster is used in galactic cluster distance measurements. This is, however, a very poorly established quantity.

In any case, beyond about  $10^8$  pc the red shift of spectral lines is available for distance measuring. This method is based on a linear relation between distance and the velocity of recession resulting from the expansion of the universe. The recession velocity of a source is determined from the Doppler shift (toward the red) of characteristic lines in its spectrum. (This method is not very useful below  $10^8$  pc, where random motions mask the motion of cosmic expansion.) The distance versus velocity relation also serves to place a boundary on the observable universe at that distance at which the recession velocity goes to the speed of light and emitted radiation is red shifted away altogether. This distance is about  $4 \times 10^9$  pc depending on the true value of Hubble's constant of proportionality between distance and recession velocity.

#### Accuracy of Intensity Distance Measurements

There are poorly defined sources at all ranges, for which intensity distance measurements are not very useful (e.g., non-main sequence stars in our own galaxy, or quasars and individual galaxies at very great



distances). Also, each step in the intensity distance ladder gets less precise, partly because it is calibrated using an increasing number of uncertain lower steps, and partly because it is based on the comparison of sources of increasingly less well defined absolute magnitude.

At the galactic cluster distance measurement level, for example, the following are just a few of the reasons for inaccuracy. Galaxies are first of all not spherical, and so they present various aspects to the observer. Also, since they have no well defined boundary, there is a variety of possible ways of defining their intensities. (This is discussed in the section covering point sources in Appendix C.) The evidence is not strong that there is in fact a physical limit to the absolute magnitude of galaxies, and that if there is, that at least one member of every cluster can be expected to attain it. In an effort to use a quantity more in line with those of the more meaningful mean value type, some astronomers arbitrarily use the fifth brightest galaxy in an attempt to avoid the statistically poorly behaved extreme values. (Using the mean itself is problematic because in more distant clusters fewer members are bright enough to be detected, causing a shift in the mean value.) There is even the question of whether typical galaxies of today are the same as their counterparts were billions of years ago when the light received from the most distant sources was emitted. In view of all these uncertainties, it is not surprising that beyond  $10^8$  pc intensity methods serve mainly to offer statistical support for the general interpretation of red shift measurements.

As stated previously, the accuracy of intensity distance measurements is not the same in all distance regimes. In order to draw

any conclusions regarding the impact of calculated gravitational changes on intensity distance measurement, then, one must make a quantitative estimate of the accuracy otherwise involved in such measurements at various ranges.

Precision is not considered since errors in the actual intensity measurements are insignificant compared to the other uncertainties involved. On the other hand, there may be theoretical errors (aside from that considered here) in the inverse square distance relation, or other unknowns such as absorption by dust and gas, whose magnitudes are altogether unknown. The only factor considered in estimating the level of accuracy involved with distance measurements, therefore, will be the ability to accurately characterize sources, and even there, an optimistic, limiting highest accuracy will be roughly chosen.

It is seen in the earlier discussion that while intensity distance measurements are made at all ranges, their accuracy decreases with increasing distance. Therefore, the minimum fractional change in intensity due to gravitational fields that would have a significant impact on distance determinations increases with the distance involved. The intensities of the nearest stars, measured for calibration purposes, are generally not given much more precisely than to within a percent, since there is no need to be any more accurate than the associated parallax distance measurement. A one percent change in intensity is therefore taken as the threshold level of significance for sources within the Milky Way. On the other hand, at the limits of the observable universe, even a gravitationally induced intensity change of the order of the intensity itself would not be especially noteworthy in view of

the uncertainties already present. In the intermediate range, for the distances to other galaxies in which individual stars can be resolved, a 10 percent change in intensity will be taken to be minimally significant. We therefore have a rough standard for interpreting the significance with regard to distance measurements, of the gravitational intensity changes to be calculated.

#### Worst Case Scenarios

In order to place an upper limit on the magnitude of the statistical intensity variations that can be expected, three "worst case" scenarios are examined. These are those situations from across the full range of intensity distance measurements, in which the possibility of large statistical mean gravitational intensity variations seems the greatest. They are:

1. Sources at or beyond the far edge of the Milky Way, observed through the field of deflecting stars in the galactic plane.

2. Resolvable sources observed through the maximum dimension of other galaxies. (It is assumed that it would be difficult to accurately separate the intensity contributions of two galaxies directly in line with the observer. Therefore, this scenario is limited to resolvable sources within the far side of the galaxy of deflecting stars.)

3. The most remote galaxies, observed through the universal distribution of galaxies.

The actual population of deflecting masses is examined in each of these scenarios to determine the validity of approximations, and to perform the numerical evaluation of the general results.

### Pertinent Astrophysical Quantities

It is necessary for subsequent discussions to establish the values of some astrophysical quantities. Most of these values are not known very accurately and are subject to revision every time new data come in. Furthermore, many have been rounded off and idealized for this study. The exact figures, therefore, should be accepted only roughly. This is, however, sufficient for the order of magnitude level of accuracy required in this investigation.

The "standard" stellar mass,  $M_s$ , is assumed to be  $3 \times 10^{33}$  g, or about 1.5 times the sun's mass,  $M_\odot$ . The value of  $F$  for standard stars,  $F_s$ , is then  $3 \times 10^{-13}$  pc. A solar radius,  $R_\odot$ , of  $7 \times 10^{10}$  cm is assigned to all stars.

The diameter of the Milky Way is taken to be 25 kpc, with the sun located in the galactic plane but out toward one edge of the disk, about 20 kpc from the opposite side. Twenty kpc is therefore used as the largest possible distance of observation through the Milky Way, and since the Milky Way is a fairly large spiral galaxy, the same value is used as the typical maximum dimension of other galaxies. (Actually, since galaxies have no well defined boundary, their "dimensions" are somewhat arbitrary.)

The distribution of stars throughout the galaxy is not at all uniform. The stellar density decreases with distance from the galactic plane, and, in the vicinity of the sun, is down to a third of its local value by about 350 pc. There is also a gradual increase in density toward the galactic center, and Lequeux suggests that in a small central core of about a hundred parsecs it may rise steeply to a value several

thousand times that near the sun (Ref 14). Furthermore, there is the uneven distribution giving rise to the spiral arms, and the occurrence of possibly a tenth of all stars within some sort of cluster. Nevertheless, for simplicity a uniform star density is assumed at least in the vicinity of the galactic plane.

Faber and Gallagher cite several calculations indicating a stellar mass density near the sun of between  $0.05$  and  $0.09 M_{\odot} \text{ pc}^{-3}$  (Ref 15). (An additional mass of about  $0.03 M_{\odot} \text{ pc}^{-3}$  from dispersed gas and dust does not enter the treatment of ray deflection by discrete deflecting masses within the galaxy.) For the worst case analysis, looking across the galactic disk, only a relatively minor increase due to the small size of the central region of much higher density is included, and a rough mean density,  $\sigma_s$ , of  $0.1$  standard ( $1.5 M_{\odot}$ ) stars per cubic parsec is therefore assumed along that length, and the same density is assumed in the planes of other galaxies. (It might be noted, then, that most actual viewing situations will involve looking through lower star densities in addition to looking through shorter portions of the galaxy.)

On an extragalactic scale, the mass of a typical galaxy is taken to be  $10^{44} \text{ g}$ , giving a value of  $10^{-2} \text{ pc}$  for  $F_g$ . (The possible existence of "galactic coronae," currently being theorized, has not been included. Including such coronae, if they are determined to exist, could increase the typical galactic mass by up to two orders of magnitude.) The grouping of galaxies into clusters is not considered, and  $3 \times 10^{-18} \text{ pc}^{-3}$  is used as the mean density of galaxies,  $\sigma_g$  (Ref 16). Finally, the  $4 \times 10^9 \text{ pc}$  taken as the radius of the observable universe,  $R_u$ , or that

distance at which the cosmological recession velocity goes to the speed of light, is based on a value of 75km/sec/Mpc for Hubble's constant. This value is not well determined, but Hodge summarizes about 20 recent calculations using various methods, and most of the results are between 50 and 100km/sec/Mpc (Ref 17).

### III. Gravitational Index of Refraction

According to the theory of relativity, light rays travel along null geodesics in 4-space. That is, along a light path

$$(ds)^2 = g_{\alpha\beta} dx^\alpha dx^\beta = 0 \quad (3-1)$$

where  $ds$  is the 4-space path element,  $g_{\alpha\beta}$  is the metric tensor,  $dx^0 = cdt$  is the time coordinate differential and  $dx^1$ ,  $dx^2$  and  $dx^3$  the spatial coordinate differentials, and where the Einstein convention of summing over pairs of like indices, one contravariant and one covariant, has been employed.

By the standard calculations of general relativity carried out in Appendix A, the metric tensor in a weak gravitational potential field is given by Eq (A-51) as

$$g_{\alpha\beta} = \begin{pmatrix} 1 + \frac{2\Phi}{c^2} & 0 & 0 & 0 \\ 0 & -1 + \frac{2\Phi}{c^2} & 0 & 0 \\ 0 & 0 & -1 + \frac{2\Phi}{c^2} & 0 \\ 0 & 0 & 0 & -1 + \frac{2\Phi}{c^2} \end{pmatrix} \quad (3-2)$$

where  $c$  is the speed of light in a vacuum in the absence of gravity, and  $\Phi$  is the classical gravitational potential. Inserting these values into Eq (3-1) gives

$$0 = \left(1 + \frac{2\Phi}{c^2}\right)(dx^0)^2 + \left(-1 + \frac{2\Phi}{c^2}\right)\left[(dx^1)^2 + (dx^2)^2 + (dx^3)^2\right] \quad (3-3)$$

and writing this in 3-space coordinates and letting  $(d\sigma)^2 = (dx^1)^2 + (dx^2)^2 + (dx^3)^2$  gives

$$0 = \left(1 + \frac{2\Phi}{c^2}\right) c^2(dt)^2 - \left(1 - \frac{2\Phi}{c^2}\right) (d\sigma)^2 \quad (3-4)$$

Thus,

$$\frac{d\sigma}{dt} = v = c \sqrt{\frac{1 + \frac{2\Phi}{c^2}}{1 - \frac{2\Phi}{c^2}}} \quad (3-5)$$

where  $v$  is the local coordinate velocity of light in 3-space. One can, therefore, include the gravitational effects on light propagation in a vacuum in Euclidean flat space analyses by associating an index of refraction,  $n$ , with gravitational fields, using the relation

$$n \equiv \frac{c}{v} = \sqrt{\frac{1 - \frac{2\Phi}{c^2}}{1 + \frac{2\Phi}{c^2}}} \quad (3-6)$$

Since all masses are being treated as point masses, their gravitational potentials are given by

$$\Phi(\rho) = \frac{-MG}{\rho} \quad (3-7)$$

In the weak field regions considered in this analysis, condition (1-1) is met and so the quantity  $2\Phi/c^2$  is very small. Equation (3-6) can therefore be approximated by truncating its series expansion to give



$$n = 1 + \frac{2GM}{c^2 \rho}$$
$$= 1 + \frac{F}{2\rho}$$

(3-8)

Some support for the validity of this index of refraction approach is that it leads to the traditional total small angle of deflection of a ray by the gravitational field of a point mass,  $4MG/c^2 r_0$  radians, where  $r_0$  is essentially the distance of closest approach. This expression is obtained in the steps leading up to Eq (4-25) of this report by analyzing the propagation of waves in an inhomogeneous medium with an index of refraction given by Eq (3-8). The solution of the 4-space variational problem, giving the same result, is shown in Appendix B.

#### IV. Effect of a Single Deflecting Mass on Intensity

In this section, the index of refraction given by Eq (3-8) is used in finding an expression for the change in intensity due to the gravitational field of a single mass.

##### Paraxial Approach to Light Propagation

Due to the great distances between celestial objects, it is assumed that in the region being analyzed the actual incident, unperturbed spherical waves are closely approximated by plane waves. Experience shows that the deflection of light rays by gravitational fields is very small. This suggests a paraxial analysis in which a perturbed phase front is assumed to propagate in a fixed direction, but which allows the perturbation to vary as it propagates. Rays, as usual, are defined as being everywhere normal to the constant phase surfaces. Cylindrical coordinates are used to take advantage of the axial symmetry, and the lack of angular variation results in the following simplified definitions of the gradient, transverse gradient, Laplacian and transverse Laplacian, respectively.

$$\left. \begin{aligned} \nabla &= \hat{r} \frac{\partial}{\partial r} + \hat{z} \frac{\partial}{\partial z} \\ \nabla_T &= \hat{r} \frac{\partial}{\partial r} \\ \nabla^2 &= \frac{1}{r} \frac{\partial}{\partial r} \left( r \frac{\partial}{\partial r} \right) + \frac{\partial^2}{\partial z^2} \\ \nabla_T^2 &= \frac{1}{r} \frac{\partial}{\partial r} \left( r \frac{\partial}{\partial r} \right) \end{aligned} \right\} (4-1)$$

As Figure 2 shows, the axes are aligned so that the deflecting mass,  $M$ , is at the origin, and propagation is in the  $+\hat{z}$  direction. The incident plane wave is then unperturbed at  $z = -\infty$ .

The paraxial equations to be solved are then determined as follows. Substituting the general form of a monochromatic wave,

$$E(\vec{r}, t) = P(\vec{r}) e^{-i\omega t} \quad (4-2)$$

into the time dependent wave equation,

$$\nabla^2 E - \frac{n^2}{c^2} \frac{\partial^2 E}{\partial t^2} = 0 \quad (4-3)$$

produces the time independent wave equation,

$$\nabla^2 P + k^2 n^2 P = 0 \quad (4-4)$$

where  $k = \frac{\omega}{c} = \frac{2\pi}{\lambda}$ . For  $n$  nearly equal to one and propagation in the  $+\hat{z}$  direction we assume a paraxial solution of the form

$$P(r, z) = U(r, z) e^{ikz} \quad (4-5)$$

where  $U(r, z)$  varies slowly with  $z$ . Substituting this expression into Eq (4-4) and performing the differentiation gives

$$\nabla_r^2 U + \frac{\partial^2 U}{\partial z^2} + 2ik \frac{\partial U}{\partial z} + k^2 (n^2 - 1) U = 0 \quad (4-6)$$

By the assumption of a slow change in  $U$  with  $z$ , and in the geometrical optics limit where  $k \rightarrow \infty$ , the second term can be neglected, and by

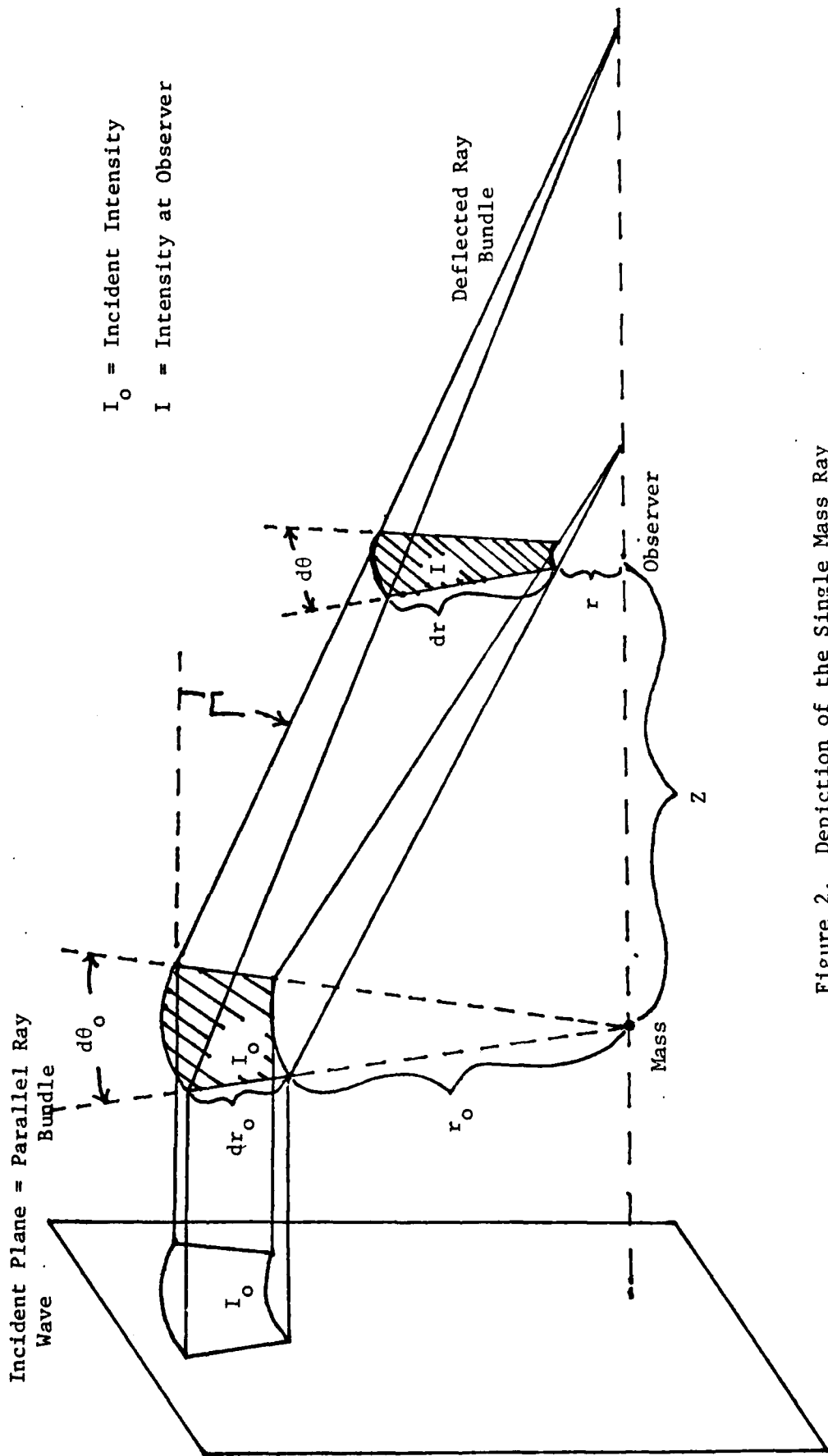


Figure 2. Depiction of the Single Mass Ray Deflection Problem

writing  $n = 1 + \tilde{n}$ ,  $|\tilde{n}| \ll 1$ , the last term is approximately  $2k^2 \tilde{n} U$ .

Thus,

$$\nabla_T^2 U + 2ik \frac{\partial U}{\partial z} + 2k^2 \tilde{n} U = 0 \quad (4-7)$$

We now rewrite the complex quantity,  $U$ , as

$$U(r, z) = A(r, z) e^{i\phi(r, z)} \quad (4-8)$$

where the amplitude  $A$  and the phase  $\phi$  are real quantities. Substituting into Eq (4-7) and separating the real and imaginary parts gives

$$\frac{\partial A}{\partial z} = \frac{1}{2k} \left[ 2 \nabla_T A \cdot \nabla_T \phi + A \nabla_T^2 \phi \right] \quad (4-9)$$

and

$$\frac{\partial \phi}{\partial z} = \frac{1}{2kA} \left[ \nabla_T^2 A - A \nabla_T \phi \cdot \nabla_T \phi \right] + k \tilde{n} \quad (4-10)$$

From Eq (4-10),  $\phi$  is evidently of order  $k$ , so the dot product is of order  $k^2$ , and the  $\frac{1}{2kA} \nabla_T^2 A$  term is neglected in the geometrical optics limit, where  $k \rightarrow \infty$ . Also, the real quantity of interest is the intensity,  $I$ , where

$$I = U^* U = A^2 \quad (4-11)$$

Therefore, substituting  $\sqrt{I}$  for  $A$ , Eqs (4-9) and (4-10) become

$$\frac{\partial I}{\partial z} = -\frac{1}{k} \left[ \nabla_T I \cdot \nabla_T \phi + I \nabla_T^2 \phi \right] \quad (4-12)$$

and

$$\frac{\partial \phi}{\partial z} = \frac{1}{2k} \nabla_T \phi \cdot \nabla_T \phi + k \tilde{n} \quad (4-13)$$

We next make a thin phase screen approximation where the entire phase change relative to an unperturbed plane wave caused by the variation of refractive index along the ray path is compressed into the  $z = 0$  plane, and  $\tilde{n}$  is set to zero elsewhere. (See discussion in Appendix C.) Thus, denoting the uniform phase of an unperturbed plane wave at  $z = 0$  by  $\phi_0$ , the approximated phase immediately to the right of  $z = 0$  is

$$\phi(r, 0^+) = \phi_0 + k \int_{-\infty}^{\infty} \tilde{n}(r, s) ds \quad (4-14)$$

where by the paraxial approximation, the integral over the ray path is carried out at constant  $r$ . Now  $\nabla_T \phi = 0$  for  $z < 0$  and

$$\begin{aligned} \nabla_T \phi(r, 0^+) &= \nabla_T \left[ k \int_{-\infty}^{\infty} \tilde{n}(r, s) ds \right] \\ &= k \int_{-\infty}^{\infty} \nabla_T \tilde{n}(r, s) ds \end{aligned} \quad (4-15)$$

or

$$\frac{\partial}{\partial r} \phi(r, 0^+) = k \int_{-\infty}^{\infty} \frac{\partial}{\partial r} \tilde{n}(r, s) ds \quad (4-16)$$

Also, since  $\tilde{n} = 0$  for  $z \neq 0$ , Eq (4-13) becomes

$$\begin{aligned}\frac{\partial \phi}{\partial z} &= -\frac{1}{2k} \nabla_T \phi \cdot \nabla_T \phi \\ &= -\frac{1}{2k} \frac{\partial \phi}{\partial r} \frac{\partial \phi}{\partial r}\end{aligned}\tag{4-17}$$

Partially differentiating both sides of this expression with respect to  $r$  and rearranging terms gives

$$\frac{\partial}{\partial z} \left( \frac{\partial \phi}{\partial r} \right) = -\frac{1}{k} \frac{\partial \phi}{\partial r} \frac{\partial}{\partial r} \left( \frac{\partial \phi}{\partial r} \right)\tag{4-18}$$

We now define a variable  $\Gamma$ , where

$$\Gamma(r, z) = \frac{1}{k} \frac{\partial}{\partial r} \phi(r, z)\tag{4-19}$$

Since the gradient of the phase

$$\begin{aligned}\nabla \phi &= \nabla_T \phi + \hat{z} \frac{\partial \phi}{\partial z} \\ &= \hat{r} k \Gamma + \hat{z} k\end{aligned}\tag{4-20}$$

defines the direction of ray propagation,  $\Gamma(r, z)$  is seen to be the tangent of the angle of deflection of the ray passing through  $(r, z)$ .

(The angle and its tangent both always being negative.)

Substituting  $\Gamma(r, z)$  into Eqs (4-18) and (4-12), our problem can now be stated as follows.

Solve

$$\frac{\partial \Gamma}{\partial z} = -\Gamma \frac{\partial \Gamma}{\partial r} \quad (4-21)$$

subject to the initial condition

$$\Gamma(r, 0^+) = \int_{-\infty}^{\infty} \frac{\partial}{\partial r} \tilde{n}(r, s) ds \quad (4-22)$$

where from Eq (3-8) and the relation,  $n = 1 + \tilde{n}$ ,

$$\tilde{n}(r, s) = \frac{2GM}{c^2 \sqrt{r^2 + s^2}} = \frac{F}{2\sqrt{r^2 + s^2}} \quad (4-23)$$

Finally, use this  $\Gamma(r, z)$  to solve

$$\frac{\partial I}{\partial z} = -\Gamma \frac{\partial I}{\partial r} - \frac{I}{r} \frac{\partial}{\partial r} (r\Gamma) \quad (4-24)$$

for  $I(r, z)$  where  $I(r, 0) = I_0$ , a constant.

#### Solution of the Paraxial Equations

From Eqs (4-22) and (4-23) comes

$$\begin{aligned} \Gamma(r, 0^+) &= \int_{-\infty}^{\infty} \frac{\partial}{\partial r} \left( \frac{F}{2\sqrt{r^2 + s^2}} \right) ds \\ &= -\frac{Fr}{2} \int_{-\infty}^{\infty} \frac{ds}{(\sqrt{r^2 + s^2})^3} \\ &= -\frac{F}{r} = -\frac{4MG}{c^2 r} \end{aligned} \quad (4-25)$$



This is the tangent of the total ray deflection angle, but since it is a very small quantity for most realizable conditions, it may equally well express the deflection angle itself. Furthermore, as a result of having made the paraxial approximation, the  $r$  in Eq (4-25) can be identified equally well with either the impact parameter or the distance of closest approach. (This expression is supported by the close agreement of its calculated value of  $8.5 \times 10^{-6}$  radians with the measured deflection of rays grazing the solar disk.)

Since all deflection is at the  $z = 0$  plane, the rays elsewhere will be straight lines and geometrical arguments lead to the following solution of Eq (4-21)

$$\begin{aligned} \Gamma(r, z) &= \Gamma(r_0(r, z), 0^+) \\ &= \frac{-F}{r_0(r, z)} \end{aligned} \quad (4-26)$$

where  $r_0(r, z)$  is the value of  $r$  at  $z = 0$  for the ray passing through  $(r, z)$ . Now

$$\begin{aligned} r(r_0, z) &= r_0(r, z) + z \Gamma(r_0(r, z), 0^+) \\ &= r_0(r, z) - \frac{Fz}{r_0(r, z)} \end{aligned} \quad (4-27)$$

but this can be solved for  $r_0$  giving

$$r_0(r, z) = \frac{r}{2} + \frac{1}{2} \sqrt{r^2 + 4Fz}$$

$$= \frac{r}{2} \left[ 1 + \sqrt{1 + \frac{4Fz}{r^2}} \right] \quad (4-28)$$

where the negative sign in the quadratic formula did not make sense for the primary image rays. Substituting  $r_0$  into Eq (4-26), gives

$$\Gamma(r, z) = \frac{-2F}{r \left[ 1 + \sqrt{1 + \frac{4Fz}{r^2}} \right]} = \frac{-8MG}{c^2 r \left[ 1 + \sqrt{1 + \frac{16MGz}{c^2 r^2}} \right]} \quad (4-29)$$

which indeed satisfies Eq (4-21).

We next look for the solution to Eq (4-24) using this value of  $\Gamma$ . This equation too, is most easily solved using geometrical arguments along with the conservation of energy. The power transmitted through a cross sectional area,  $dA_0 = r_0 d\theta_0 dr_0$ , of an incident plane wave of uniform intensity,  $I_0$ , is  $P_0 = I_0 dA_0 = I_0 r_0 d\theta_0 dr_0$ . The unequal deflection of the bounding rays of this bundle results in a change in its cross sectional area as it propagates in the  $z$  direction, but the total power remains the same. That is,  $P_0 = IdA = Ird\theta dr$ . Therefore,

$$I_0 r_0 d\theta_0 dr_0 = I r d\theta dr \quad (4-30)$$

Clearly, all rays remain in the plane determined by their initial path and the deflecting mass. Hence, there is no change in  $\theta$  and  $d\theta = d\theta_0$ . Equation (4-30) thus gives

$$I = I_0 \frac{r_0}{r} \frac{dr_0}{dr} \quad (4-31)$$

Now  $r_0$  is given by Eq (4-28), and from it,

$$\begin{aligned} dr_0 &= \frac{1}{2} \left[ dr + \frac{2r dr}{2\sqrt{r^2 + 4Fz}} \right] \\ &= \frac{dr}{2} \left[ \frac{1 + \sqrt{1 + \frac{4Fz}{r^2}}}{\sqrt{1 + \frac{4Fz}{r^2}}} \right] \end{aligned} \quad (4-32)$$

Equation (4-31) then becomes

$$\begin{aligned} I(r, z) &= I_0 \frac{r}{2} \left[ 1 + \sqrt{1 + \frac{4Fz}{r^2}} \right] \frac{dr}{2} \left[ \frac{1 + \sqrt{1 + \frac{4Fz}{r^2}}}{\sqrt{1 + \frac{4Fz}{r^2}}} \right] \\ &\quad \underline{\hspace{10em} r dr} \\ &= I_0 \frac{\left[ 1 + \sqrt{1 + \frac{4Fz}{r^2}} \right]^2}{4 \sqrt{1 + \frac{4Fz}{r^2}}} \end{aligned} \quad (4-33)$$

an expression which indeed satisfies Eq (4-24) with  $\Gamma$  given by (4-29), and gives the change in intensity due to the gravitational field of a single mass.

Equation (4-33) may appear objectionable because it is always positive, and when integrated over an infinite plane it does not appear

to result in conservation of energy in the whole, even excluding the singularity at  $r = 0$ . This is not unexpected, however, since it arises from integrating the incident uniform plane wave over an infinite extent and attempting to compare infinite quantities when it is only locally that the plane wave approximation is justified (as in Appendix C). In a more detailed solution using a point source and spherical waves one would expect an increase in intensity on the side toward the deflector to be balanced by a decrease in intensity in the direction away from the deflector. (In obtaining such a solution one would have to abandon the approximation of integrating rays from  $-\infty$  to  $+\infty$ , as well as the plane wave approximation.)

V. Approximation of the Single Mass Intensity  
Expression, and Its Validity

In this section, an approximation to expression (4-33) for the intensity change is made and justified.

Approximation for  $r^2 \gg 4MGz/c^2$

The form of Eq (4-33), in spite of all the approximations made in deriving it, is still not suitable for a simple statistical analysis. It can be further simplified, however, if

$$r^2 \gg Fz = \frac{4MGz}{c^2} \quad (5-1)$$

We recall that the first three terms of the Maclaurin expansion of  $\sqrt{1+x}$ , for small  $x$ , are

$$\sqrt{1-x} \simeq 1 + \frac{x}{2} - \frac{x^2}{4} \quad (5-2)$$

Using this, Eq (4-33) can be expanded in terms of the small quantity,  $4Fz/r^2$ , to give

$$I \simeq \frac{I_0}{4} \frac{\left[ 2 + \frac{2Fz}{r^2} - 2\left(\frac{Fz}{r^2}\right)^2 \right]^2}{\left[ 1 + \frac{2Fz}{r^2} - 2\left(\frac{Fz}{r^2}\right)^2 \right]}$$

$$\simeq I_0 \frac{\left[ 1 + \frac{2Fz}{r^2} - \left(\frac{Fz}{r^2}\right)^2 + \dots \right]}{\left[ 1 + \frac{2Fz}{r^2} - 2\left(\frac{Fz}{r^2}\right)^2 \right]}$$

$$\simeq I_0 \left[ 1 + \left( \frac{Fz}{r^2} \right)^2 + \dots \right]$$

$$\simeq I_0 \left[ 1 + \left( \frac{4MGz}{c^2 r^2} \right)^2 \right]$$

(5-3)

(This same expression can be obtained by assuming condition (5-1) at any earlier point in Chapter IV. When this is done, straightforward mathematical procedures can be employed from that point on, without falling back on geometrical arguments. It is convenient in such calculations to work with the log amplitude,  $\chi$ , where  $I = e^{2\chi}$ , and discard the first term on the right side of Eq (4-24), which is valid for  $r^2 \gg 4Fz$ .)

Although there is no uniformity of approach or choice of variables and approximations, the simplified expression (5-3) is functionally similar to expressions previously derived by others (e.g., Ref 18). Looking at either this expression or expression (4-33), it would seem that for a sufficiently perfect alignment of source and deflector, virtually limitless magnification of intensity could occur. The results using real extended sources and deflecting masses would not be expected to exhibit such perfect singularities, but very large magnifications should indeed still be possible.

It should be noted that while both expressions (4-33) and (5-3) give intensity amplifications that go to infinity as  $r$  goes to zero, their behavior is quite different in this limit. As  $r^2$  becomes smaller

relative to  $Fz$ , expression (5-3) begins to consistently err on the high side. And in the limit  $r^2 \ll Fz$ , expression (4-33) approaches the asymptotic form  $I_0(Fz/2r)$ , whereas expression (5-3) becomes  $I_0(F^2 z^2 / r^4)$ , giving results which can be many orders of magnitude too large.

Applicability of the Condition  $r^2 \gg 4MGz/c^2$

It is next shown that assuming condition (5-1) for deflecting masses is reasonable in view of the actual deflector populations in the three worst case scenarios. Clearly, for a given deflector and incident plane wave, for any particular value of  $r$ , there is some distance down stream beyond which the intensity expression (5-3) based on condition (5-1), is invalid.

To be more precise, one can rewrite Eq (5-1) as

$$r^2 > w F z \tag{5-4}$$

where the proportionality constant,  $w$ , is a parameter determined from the minimum acceptable fractional error in the calculations of intensity. Since each of the three scenarios has its own associated level of accuracy, a different value of  $w$  is appropriate for each one. When  $r^2 = 6Fz$ , the difference between the intensity changes calculated from Eqs (4-33) and (5-3) is one percent of the actual observed intensity. In view of the one percent level of accuracy used for scenario one, six is therefore taken as the value of  $w$  appropriate for that scenario. A value of 2.5 for  $w$  gives a maximum relative error of 9.6 percent, so that value is adopted for the second scenario. In the third scenario,  $w$  is taken as one, which gives a maximum error of 56 percent.

In each case, then, Eq (5-4) defines a paraboloid with the deflector at the vertex, within which the errors resulting from the use of expression (5-3) for the intensity would be unacceptably large. The radius, at a distance  $z$ , of these "restricted" paraboloids is, therefore,

$$r_p(z) = \sqrt{wFz} \quad (5-5)$$

These paraboloids are also surfaces of constant change in intensity. Using the adopted values of  $w$ , the actual fractional changes (from Eq (4-33)), are about 2 percent of the incident intensity in scenario one ( $r^2 = 6Fz$ ), 6 percent in scenario two ( $r^2 = 2.5Fz$ ), and 17 percent in scenario three ( $r^2 = Fz$ ).

Assuming a standard mass for all deflectors within a scenario, it can be seen (Figure 3) that for a given observer this same paraboloid (but oppositely directed) bounds the region of possible deflector positions for which condition (5-4) is satisfied. If it can be shown that for a given source and observer there is a negligible chance of a deflector lying within this paraboloid, then expression (5-3) can reasonably be applied to all deflectors without introducing more than the specified acceptable error in the statistical results.

The volume,  $V_p$ , of that portion of such a paraboloid within which deflecting masses might lie, is given in general by

$$\begin{aligned} V_p &= \int_{z_1}^{z_2} \int_0^{r_p(z)} \int_0^{2\pi} r d\theta dr dz \\ &= \frac{w\pi F}{2} (z_2^2 - z_1^2) \end{aligned} \quad (5-6)$$



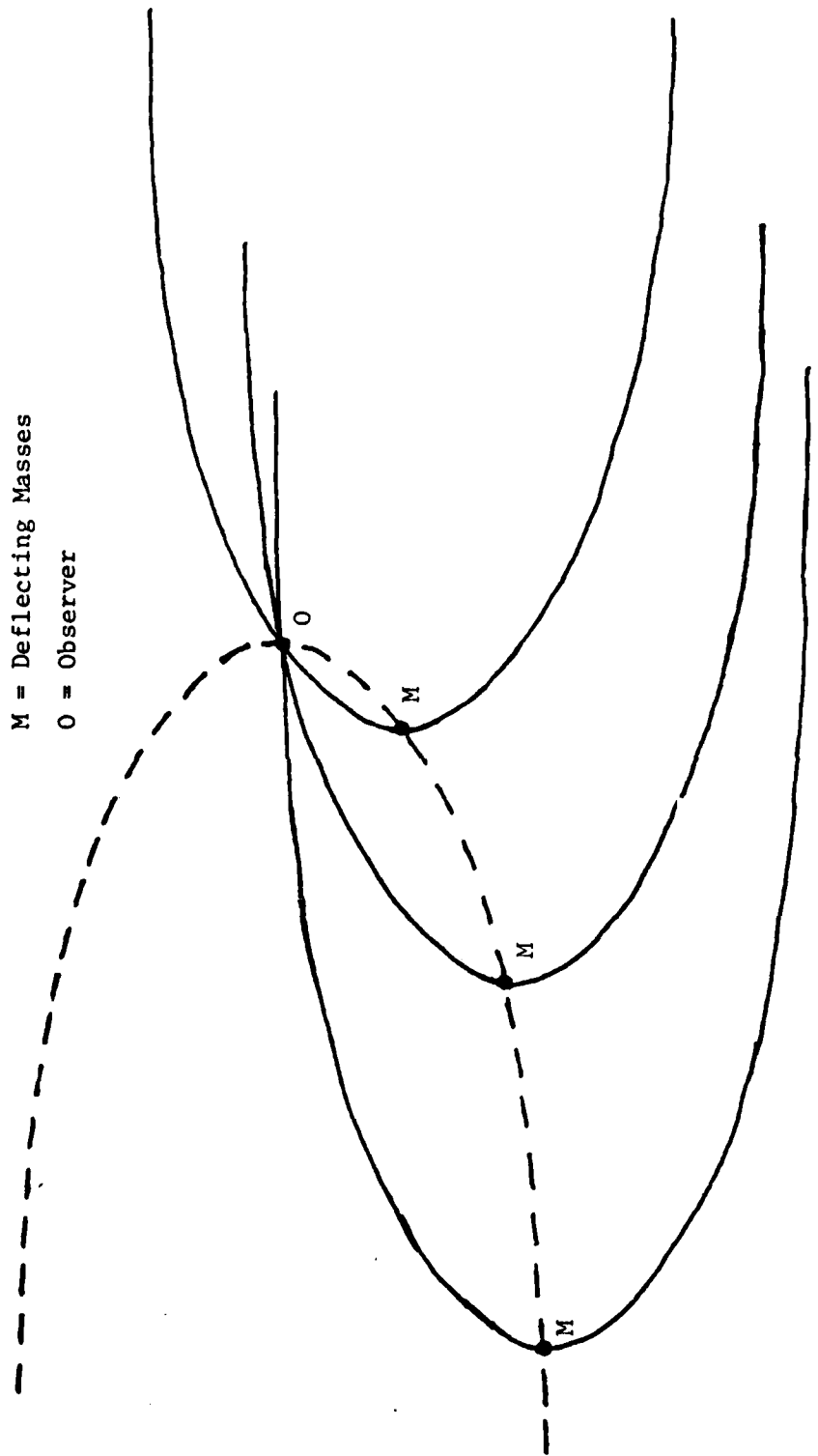


Figure 3. Cross Section of the Paraboloidal Region Restricted to Deflecting Masses Obeying Condition (5-4) for a Given Observer

where  $z_1$  and  $z_2$  are the distances at which the line of sight enters and exits the distribution of deflectors (with  $z_1$  being no less than zero, and  $z_2$  no greater than the source distance). The probable number of deflectors,  $p$ , within the "restricted" paraboloid is then given by

$$p = \sigma V_p \quad (5-7)$$

where  $\sigma$  is the density of deflectors. The validity of a blanket application of (5-3) can therefore be demonstrated for each of the three worst case scenarios by evaluating expression (5-7) using appropriate distances and populations.

Observation of Distant Sources through the Milky Way. The maximum dimension of the Milky Way through which sources might be viewed is 20 kpc, the distance to the far edge of the galaxy. From Eq (5-6), using  $z_1 = 0$ , the paraboloidal volume in this worst case is

$$\begin{aligned} V_{pg} &= \frac{6\pi F_s}{2} (2 \times 10^4 \text{ pc})^2 \\ &= 1.1 \times 10^{-3} \text{ pc}^3 \end{aligned} \quad (5-8)$$

Using this and a mean density of stars within the region of  $0.1 \text{ pc}^{-3}$  in Eq (5-7) gives

$$\begin{aligned} p &= \sigma V_{pg} \\ &\simeq 10^{-4} \text{ stars} \end{aligned} \quad (5-9)$$

That is, in this scenario there is a one in ten thousand chance of there being any deflectors individually causing more than 1.6 percent change

in the intensity of a given "worst case" source, and not having that changed intensity given within 1 percent by Eq (5-3).

In considering this figure, four things should be kept in mind:

1. For more typical cases of viewing sources through a smaller portion of the distribution of deflecting masses, the paraboloidal volume is apt to be orders of magnitude smaller. Also, the mean density of stars along the line of sight is lower for sources which are not viewed across the galactic disk. Therefore, the probability of condition (5-4) not holding for all deflectors will in most situations be much smaller than the worst case probability.

2. The error arising from using expression (5-3) for the intensity increases gradually as a deflector penetrates the paraboloid. Therefore, the intensity changes due to many of the deflectors which might lie within the paraboloid would still be reasonably well represented by expression (5-3). And in any case, the results of Eq (5-3) err on the high side so that any final results obtained from it can still be considered as an upper limit to the real results.

3. Even in those particular instances where there are deflectors sufficiently well aligned with the source that their intensity effects are not correctly given by (5-3), their contributions are added to the correct contributions from billions of other deflectors in arriving at the total effect.

4. In determining the overall mean intensity change, such possibly erroneous total effects are averaged in with those from cases where no deflectors violate condition (5-4). (In this scenario, for example, only one total effect in every ten thousand averaged in the

mean, is apt to include any erroneous individual contributions.)

In view of these considerations, there seems to be no reason why expression (5-3) cannot be assumed for all deflecting stars in this scenario.

It might also be noted that the radius of the bounding paraboloid at the far edge of the galaxy, from Eq (5-5), is only  $1.9 \times 10^{-4}$  pc (or 38 A.U.). At that distance, a deflector on the paraboloid would have an angular separation from the source of about .002" arc, which would not be resolved in the photographic plates from current telescopes. In fact, using a minimum resolvable separation of .02", no stellar mass deflector beyond about 180 pc, and only a fraction of those closer in, which produce an intensity change in varying by more than 1 percent from that calculated from expression (5-3) (and which cause more than a 2 percent intensity change), could be distinguished from the source itself (Figure 4). Therefore, any error in the statistical analysis resulting from expression (5-3) not being completely valid, should be no larger than the more fundamental error due to unresolved sources and deflectors being treated as single sources. (The diffraction limited minimum resolvable angular separation, using the Rayleigh criterion, is given by  $1.22\lambda/d$ . For the largest telescope diameter, ( $d = 5m$ ) and observation in violet light, ( $\lambda \approx 4000\text{\AA}$ ) this gives  $10^{-7}$  rad or 0.02" arc. Atmospheric effects, however, degrade actual performance from this.

Actually, using other methods, it might well be possible to recognize cases of nearly overlapping sources. Analyzing the spectrum, which must be done in any case to identify the spectral type and thereby determine the intrinsic brightness, and identifying the superimposed,

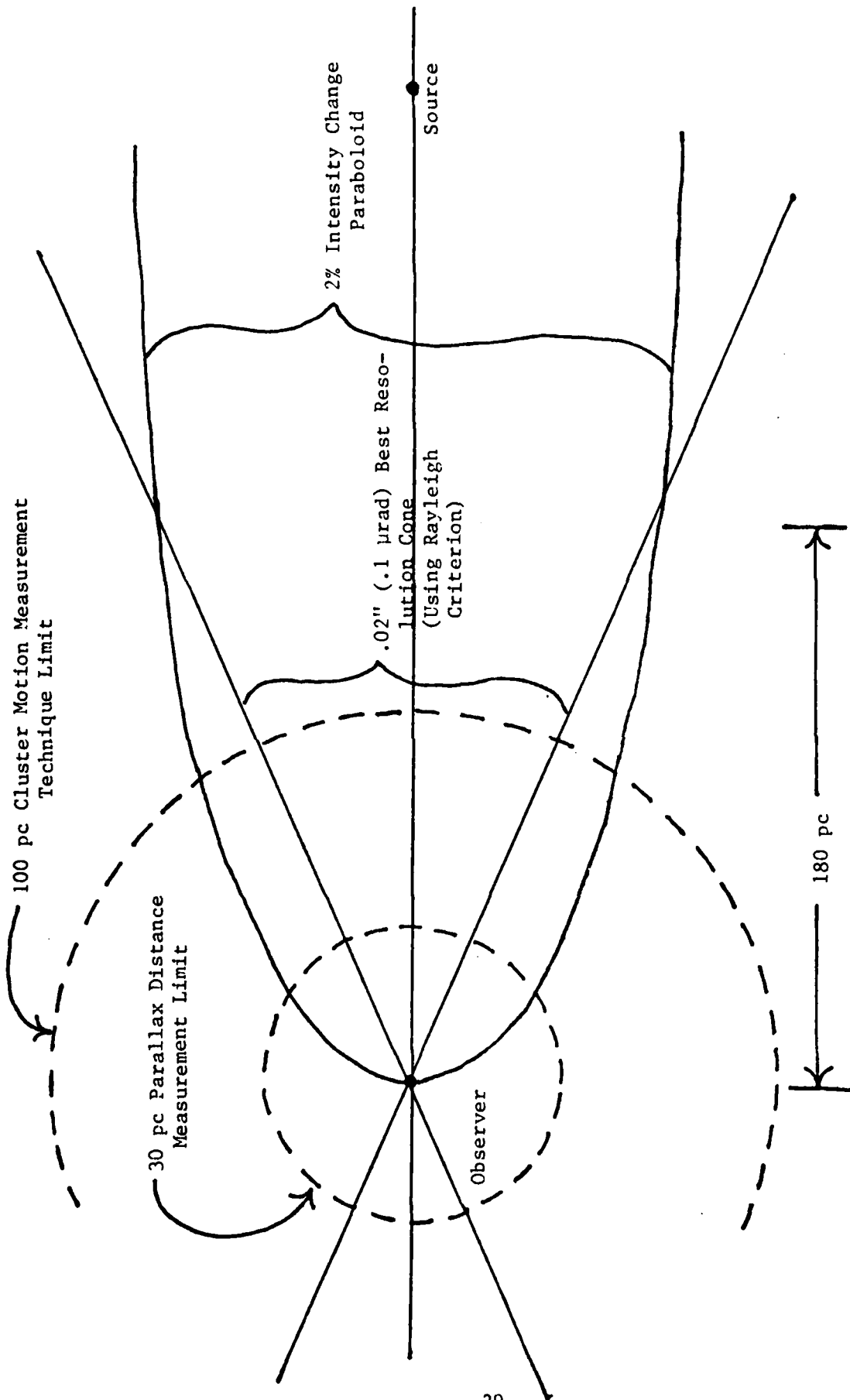


Figure 4. Comparison of the Region of Unresolved Stellar Deflecting Masses with the Region of Masses Causing More than a 2% Intensity Change

characteristic patterns of spectral lines of different types of stars can indicate the presence of multiple sources. Interferometric techniques can also be used and procedures exist for both optical and radio sources. Optical telescope apertures separated by fifty meters have been used to resolve angular dimensions of 0.003" arc (Ref 19). The much longer radio wavelengths result in vastly greater fringe separation, but the ability to make and record simultaneous measurements thousands of miles apart for later joint playback results in equally high resolution (Ref 10). It is not feasible however to perform such investigations on every source. And even when such methods do identify multiple sources, it still remains to accurately separate the intensity contributions of each. Furthermore, such sources would then be flagged as appropriate cases to analyze for large individual gravitational intensity changes.

Observation of Stars Through Other Galaxies. In the second scenario a resolvable star is viewed through part of another galaxy. Although such sources are most likely to be found in the outer regions of an elliptical or an obliquely viewed spiral galaxy, the worst case, in which a star is viewed through the full galactic diameter, is nevertheless considered.

Individual stars can be observed at a maximum range of about  $10^8$  pc. At that distance, the radius of the paraboloid bounding those masses with an intensity change given within  $.1I_0$  by Eq (5-3) is calculated from Eq (5-5), using 2.5 for  $w$ , to be less than .01 pc. The portion of galaxy bounded by it is very nearly a cylinder with that

radius and a height equal to the galactic diameter. Across a diameter of 20 kpc, its volume is then about  $5 \text{ pc}^3$ , and the mean stellar density of  $0.1 \text{ pc}^{-3}$  suggests that there is about a 50 percent probability of finding a deflector within this restricted region.

The blanket application of Eq (5-3) is certainly more questionable here than in the previous scenario. However, it is again true that this is a very extreme worst case, and the same four points listed in the previous scenario should be considered. Taken together, these considerations suggest that the error in the final results should be in keeping with the 10 percent level of accuracy optimistically associated with defining the intrinsic brightness of brightest stars or typical globular clusters of a galaxy. Therefore, in this scenario too, expression (5-3) is assumed to adequately describe the intensity effects of all deflecting masses. (Also, due to the greater distances involved, the comments under the previous scenario about errors due to unresolved sources and stellar mass deflectors are even more applicable in this scenario, and apply to deflectors well outside the 2 percent intensity change paraboloid.)

Observation of Remote Galaxies Through the Universal Distribution of Galaxies. The third scenario was that in which the random gravitational fields of entire galaxies acted on the intensities of the most distant galaxies. Proceeding as before, the worst case source is located at the edge of the observable universe (and the observer necessarily at the center). Setting  $w$  equal to one, for a maximum intensity change error of 56 percent, using the universal radius of  $4 \times 10^9 \text{ pc}$  for  $z_2$ , and setting  $z_1$  equal to zero in Eq (5-6), gives a universe

scale paraboloidal volume,  $V_{pu}$ , of

$$\begin{aligned} V_{pu} &= \pi F_g (R_u)^2 \\ &= 5 \times 10^{17} \text{ pc}^3 \end{aligned} \tag{5-10}$$

A uniform distribution of  $3 \times 10^{-18}$  galaxies per cubic parsec in Eq (5-7) suggests that probably one or two deflecting galaxies would be in a position to individually cause more than a 17 percent intensity change in a given source, and to have those intensities, as given by Eq (5-3), be in error by more than 56 percent.

The four considerations listed under the first scenario again apply, however, except that the density of the distribution of galaxies is taken to be isotropic. Since the level of accuracy associated with this scenario is roughly only to the order of magnitude, the blanket use of expression (5-3) for all deflectors again seems acceptable. It might be noted, however, that in contrast to stars, deflecting galactic masses causing up to an order of magnitude increase in intensity would be far enough displaced from the line of sight to be resolvable, even at the distance to the edge of the observable universe.

In summary, then, in view of the objective of this study, and the level of accuracy associated with intensity distance measurements in each scenario, it seems reasonable to adopt expression (5-3) as the gravitational intensity change due to all individual deflectors in all scenarios, especially since any results obtained using expression (5-3) will err on the high side in intensity, and even these too high values



will, in most cases, be negligibly small. It is also seen that, in the first two scenarios, large errors in intensity measurements are at least as likely to result simply from a failure to resolve separate sources as from the gravitational magnification associated with a nearly aligned source and deflecting mass (although the latter offers the possibility of much larger errors.)

## VI. Statistical Analysis

### Total Intensity Change Due to Many Deflectors

It is shown in Appendix C that one can ignore the deviation from straight line paths of real ray paths through actual distributions of deflecting masses. As a result of this paraxial approximation, the effects of each individual gravitational field on the intensity can be considered independent. That is, each mass has the effect of multiplying the intensity that would be observed in the presence of all other deflectors, by its own individual intensity change, as given by expression (5-3). The total intensity in the fields of N deflectors,  $I_T$ , is then expressed by the product

$$I_T = I_0 \prod_{i=1}^N \left( 1 + \frac{F_i^2 z_i^2}{r_i^4} \right) \quad (6-1)$$

where  $I_0$  would be the intensity in the absence of any gravitational perturbations.

Assuming standardized deflecting masses within a scenario, so that  $F_i = F$ , Eq (6-1) can be written out as

$$\begin{aligned} I_T &= I_0 \left[ 1 + \sum_{i=1}^N \frac{F^2 z_i^2}{r_i^4} + \sum_{i=1}^{N-1} \sum_{j=i+1}^N \frac{F^2 z_i^2}{r_i^4} \frac{F^2 z_j^2}{r_j^4} + \dots \right] \\ &= I_0 \left[ 1 + \sum_{i=1}^N \frac{F^2 z_i^2}{r_i^4} + \sum_{i=1}^{N-1} \left( \frac{F^2 z_i^2}{r_i^4} \sum_{j=i+1}^N \frac{F^2 z_j^2}{r_j^4} \right) + \dots \right] \end{aligned} \quad (6-2)$$

If the first order term,  $\sum_{i=1}^N \frac{F^2 z_i^2}{r_i^4}$ , is smaller than one by some factor, then each higher order term will be smaller than its preceding term by some larger factor (larger since the sums over smaller indicial ranges, of positive individual contributions, give smaller totals). It is assumed that the first order correction is very small compared to one, so that the higher order terms can be neglected. The total intensity can then be written simply as

$$I_T = I_o \left( 1 + F^2 \sum_{i=1}^N \frac{z_i^2}{r_i^4} \right) \quad (6-3)$$

an expression which is easily employed in the statistical calculations. Obviously, if the total fractional perturbation were not small, then the simplification to expression (6-3) could not be made, but it is shown in the end that in all real scenarios this first order total perturbation is indeed small, thereby justifying discarding the higher order terms.

#### Mean Gravitational Intensity Change

We next consider the region of space bounded by two coaxial cylinders as depicted in Figure 5. Their axes lie along the line connecting a particular source and observer, and they extend along that portion of the line of sight passing through the region throughout which deflecting masses are distributed. Their length,  $\Delta z$ , is then no larger than the source to observer distance, and may be much smaller if deflectors are distributed throughout only a fraction of the intervening space. The radius of the outer cylinder,  $R$ , is the radius of the largest

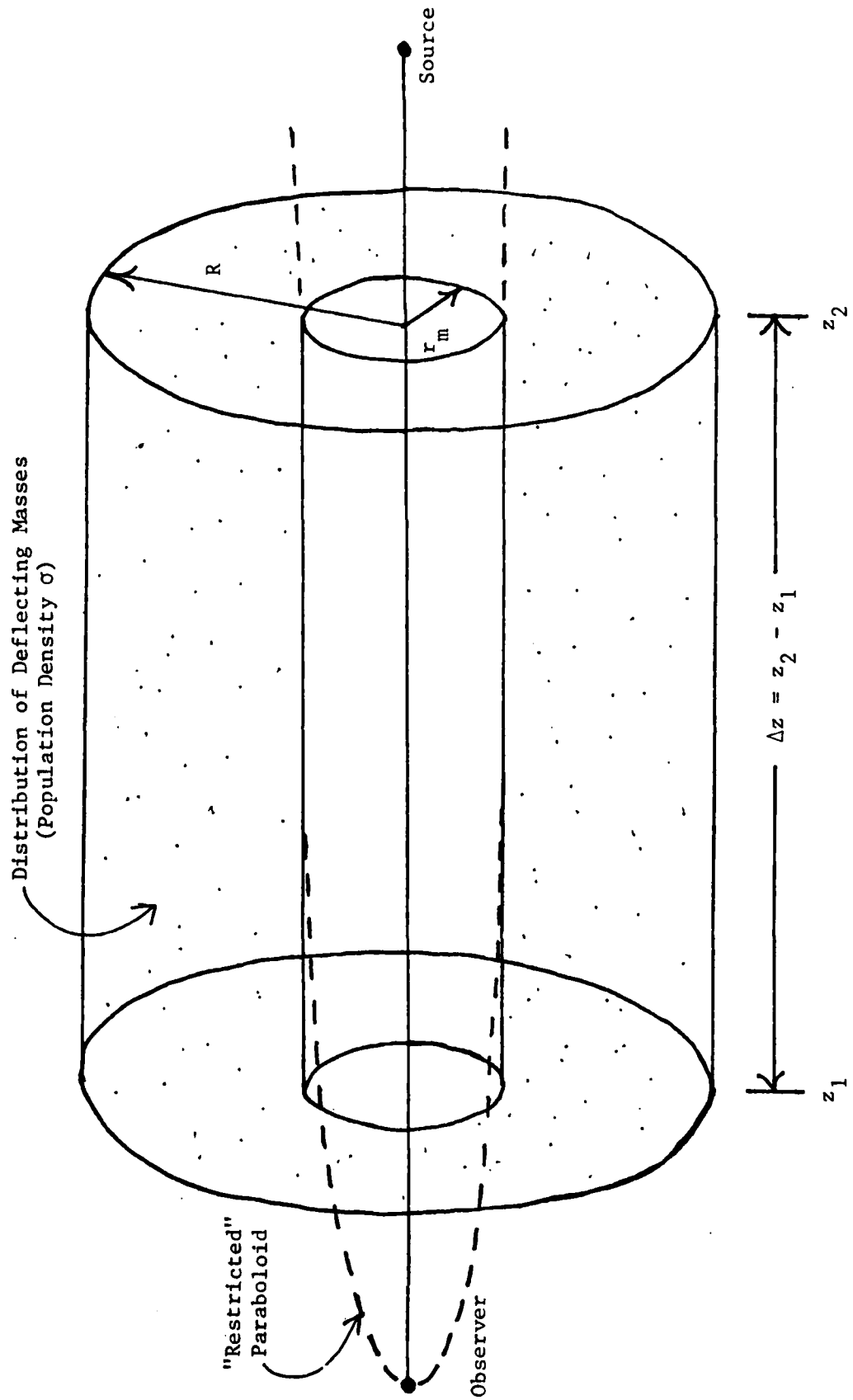


Figure 5. Geometry of the Limited Region Considered to Contain Deflecting Masses

cylinder that does not extend radially outward from the line of sight beyond any boundary of the region of deflectors.

The region within the inner cylinder is excluded in order to avoid the infinite values which result from using zero as the lower limit in several integrals. As far as the statistics are concerned, any nonzero inner radius,  $r_m$ , will keep the results finite, so that its value can be made small enough that no deflecting masses are apt to lie within the excluded cylinder, and any contributions from the region within it can be ignored. In order to avoid excessively, erroneously high results, however, the region in which expression (5-3) for the intensity is valid places a lower limit on suitable values of  $r_m$ . This lower limit is the paraboloidal radius,  $r_p$ , given by Eq (5-5), evaluated at the greatest distance along the line of sight from the observer, at which deflectors occur. This distance may be as large as the source distance, or it might be much less, depending on where the deflectors are located. In fact, using this minimum value of  $r_m$ , in all real situations the volume of the inner cylinder is only fractionally larger than the volume of the segment of the restricted paraboloid within it. Thus, since the paraboloids in each scenario have been shown to contain few deflectors, the same can be said of this smallest suitable inner cylinder, and intensity change contributions from the region within it can be either ignored or considered separately.

As an aside, one might question whether artificially excluding an inner cylinder would have been necessary if Eq (4-33) could have been retained in its unapproximated form throughout the calculations. And in fact, looking at its asymptotic form for  $r^2 \ll Fz$ , wherein the intensity

becomes proportional to  $\sqrt{Fz}/r$ , it is seen that there would indeed be no problem with  $r_m$  being zero in evaluating the mean intensity change, since in the calculations corresponding to those steps leading up to Eq (6-9), letting  $r_m$  equal zero when evaluating the integral would not give an infinite result. The problem would persist, however, in evaluating the root mean square intensity change. There would be a quantity  $\langle z_i/r_i^2 \rangle$  to be evaluated in a calculation corresponding to that preceding Eq (6-19), and letting  $r_m$  equal zero there would still produce an infinite result. Furthermore, it remains to be able to perform the calculations using expression (4-33) as it is, to give valid results for all values of  $r$ .

Using the approximate expression (5-3) is, however, sufficient and appropriate for the task at hand, which is to evaluate the total effect of all poorly aligned deflectors. It has been shown that in a given instance, there are apt to be at most a very few deflectors for which Eq (5-3) is not sufficiently precise, and it would not be difficult to analyze the effects of these few masses individually using expression (4-33). We return, therefore, to the calculations, and proceed using expression (6-3), which is itself based on Eq (5-3), for the total observed intensity of a source with unperturbed intensity,  $I_0$ .

On the basis of real dimensions in the three scenarios, one can assume that  $r_m \ll R$ , even for values of  $r_m$  much larger than the minimum suitable ones. This simplifies several expressions, one of which relates  $N$  to the population density,  $\sigma$ .  $N$ , which appears in Eq (6-3), is the total number of deflectors distributed between the cylinders, and is given by

$$\begin{aligned}
N &= \sigma (\pi R^2 \Delta z - \pi r_m^2 \Delta z) \\
&= \pi (R^2 - r_m^2) \sigma \Delta z \\
&\approx \pi R^2 \sigma \Delta z
\end{aligned} \tag{6-4}$$

The mean observed intensity for a given source, averaged over all possible distributions of gravitational deflectors within the cylinders, is the same as the sum of the mean individual effects of all the deflectors averaged over all of their possible positions within the cylinders. Using the symbol  $\langle \rangle$  to denote a spatial mean, it can be written

$$\begin{aligned}
\langle I_{\uparrow} \rangle &= I_0 \left\langle 1 + F^2 \sum_{i=1}^N \frac{z_i^2}{r_i^4} \right\rangle \\
&= I_0 \left[ \langle 1 \rangle + F^2 \sum_{i=1}^N \left\langle \frac{z_i^2}{r_i^4} \right\rangle \right] \\
&= I_0 \left[ 1 + N F^2 \left\langle \frac{z_i^2}{r_i^4} \right\rangle \right]
\end{aligned} \tag{6-5a}$$

$$= I_0 \left[ 1 + \pi R^2 \sigma \Delta z F^2 \left\langle \frac{z_i^2}{r_i^4} \right\rangle \right] \tag{6-5b}$$

The same expression and the subsequent results are used for the mean observed intensity averaged over all possible directions to sources which would produce an unperturbed intensity,  $I_0$ , and which have deflecting masses distributed with a density,  $\sigma$ , from  $z_1$  to  $z_2$  along the line of sight.

If  $P_i(r_i, z_i)$  is the normalized probability of a deflector occupying the site identified by  $(r_i, z_i)$ , then

$$\left\langle \frac{z_i^2}{r_i^4} \right\rangle = \sum_{i=1}^N P_i \left( \frac{z_i^2}{r_i^4} \right) \quad (6-6)$$

where  $n$  is the total number of discrete sites which deflectors can occupy. But there are so many deflectors that one can assume a continuous distribution and approximate expression (6-6) by the integral expression

$$\begin{aligned} \left\langle \frac{z_i^2}{r_i^4} \right\rangle &= \frac{\iiint_V \sigma \left( \frac{z_i^2}{r_i^4} \right) dV}{\iiint_V \sigma dV} \\ &= \frac{\sigma}{N} \iiint_V \frac{z_i^2}{r_i^4} dV \end{aligned} \quad (6-7)$$

where  $dV$  is the volume element and by the uniform distribution approximation the normalized probability

$$\begin{aligned} P_i(r_i, z_i) &= \frac{\sigma dV}{\iiint_V \sigma dV} \\ &= \frac{\sigma dV}{\sigma 2\pi \Delta z \left( R^2 - \frac{r_m^2}{2} \right)} \\ &= \frac{\sigma dV}{N} \end{aligned} \quad (6-8)$$

is independent of position. In the present case, using the cylindrical coordinate volume element,  $dV = r_i d\theta_i dr_i dz_i$ , and placing primes on



integration variables, Eq (6-7) can be written

$$\begin{aligned}
 \left\langle \frac{z_1^2}{r_1^4} \right\rangle &= \frac{\sigma}{N} \int_{z_1}^{z_2} \int_{r_m}^R \int_0^{2\pi} \left( \frac{z_i'^2}{r_i'^4} \right) r_i' d\theta_i' dr_i' dz_i' \\
 &= \frac{2\pi\sigma}{N} \int_{z_1}^{z_2} z_i'^2 dz_i' \int_{r_m}^R \frac{dr_i'}{r_i'^3} \\
 &= \frac{\pi\sigma(z_2^3 - z_1^3)}{3N} \left( \frac{1}{r_m^2} - \frac{1}{R^2} \right)
 \end{aligned}
 \tag{6-9}$$

For  $R \gg r_m$ , this becomes

$$\left\langle \frac{z_1^2}{r_1^4} \right\rangle = \frac{\pi\sigma(z_2^3 - z_1^3)}{3N r_m^2}
 \tag{6-10}$$

which is independent of  $R$ . This means that as long as the narrowest dimension of the distribution of deflectors, orthogonal to the line of sight, is much larger than  $r_m$ , then the actual overall shape of the region containing deflecting masses is unimportant, and for convenience, can just as well be considered to extend to infinity. (This, of course, is a result of the rapid  $r^{-4}$  drop off in intensity effects causing the smallest  $r_i$  values to dominate.)

Using the abbreviated notation  $\Delta z^n \equiv (z_2)^n - (z_1)^n$ , Eq (6-5a) now becomes

$$\begin{aligned} \langle I_T \rangle &= I_0 \left( 1 + \frac{\pi F^2 \sigma \Delta z^3}{3 r_m^2} \right) \\ &= I_0 \left( 1 + \frac{16\pi M^2 G^2 \sigma \Delta z^3}{3 c^4 r_m^2} \right) \end{aligned}$$

(6-11)

an expression for the mean observed intensity of sources of unperturbed intensity,  $I_0$ , viewed through a distance,  $L$ , of deflectors of mass,  $M$ , and distribution density,  $\sigma$ . The mean deviation in intensities,  $D_I$ , is then

$$\begin{aligned} D_I &= \langle I_T \rangle - I_0 \\ &= I_0 \frac{\pi F^2 \sigma \Delta z^3}{3 r_m^2} \\ &= I_0 \left( \frac{16\pi M^2 G^2 \sigma \Delta z^3}{3 c^4 r_m^2} \right) \end{aligned}$$

(6-12)

and is evidently very sensitive to the values  $z_1$  and  $z_2$  and the rather artificial value,  $r_m$ .

This expression can be specialized to the particular scenarios. In the cases of deflection by stars of the Milky Way and deflection by galaxies as a whole, the distribution of deflecting masses extends in to the observer, so that  $z_1 = 0$  and  $\Delta z^3 = (z_2)^3$ . For the first and third scenarios, then, Eq (6-12) can be written

$$\begin{aligned}
D_I &= \frac{I_0 F^2 \pi \sigma (z_2)^3}{3 r_m^2} \\
&= I_0 \left( \frac{16 \pi M^2 G^2 \sigma (z_2)^3}{3 c^4 r_m^2} \right)
\end{aligned}
\tag{6-13}$$

In the case of deflection by stars in other galaxies, both  $z_1$  and  $z_2$  are much greater than  $\Delta z = z_2 - z_1$ . Thus, the  $\Delta$  behaves as a differential operator, and  $\Delta z^3 = 3z^2 \Delta z$ . In the second scenario, therefore, Eq (6-12) becomes

$$\begin{aligned}
D_I &= \frac{I_0 F^2 \pi \sigma z^2 \Delta z}{r_m^2} \\
&= I_0 \left( \frac{16 \pi M^2 G^2 \sigma z^2 \Delta z}{c^4 r_m^2} \right)
\end{aligned}
\tag{6-14}$$

where  $z$  is the distance to the galaxy and  $\Delta z$  is the depth of the source into it.

#### Variance in the Distribution of Intensities

In describing the distribution of intensities about the mean, it is useful to use the variance, or mean square deviation in the intensity,  $(D_{2I})^2$ . The root mean square (r.m.s.) change,  $D_{2I}$  itself, is indicative of how well the mean change represents the typical change. In general

$$(D_{2I})^2 = \langle (I_T - \langle I_T \rangle)^2 \rangle
\tag{6-15}$$

Using expressions (6-3) and (6-11) it becomes

$$\begin{aligned}
(D_{2I})^2 &= \left\langle \left[ I_0 \left( 1 + F^2 \sum_{i=1}^N \frac{z_i^2}{r_i^4} \right) - I_0 \left( 1 + F^2 \frac{\pi \sigma \Delta z^3}{3 r_m^3} \right) \right]^2 \right\rangle \\
&= I_0^2 F^4 \left\langle \left( \sum_{i=1}^N \frac{z_i^2}{r_i^4} - \frac{\pi \sigma \Delta z^3}{3 r_m^3} \right)^2 \right\rangle \\
&= I_0^2 F^4 \left[ \left\langle \left( \sum_{i=1}^N \frac{z_i^2}{r_i^4} \right)^2 \right\rangle - \frac{2 \Delta z^3 \sigma \pi}{3 r_m^3} \left\langle \sum_{i=1}^N \frac{z_i^2}{r_i^4} \right\rangle + \frac{\pi^2 (\Delta z^3)^2 \sigma^2}{9 r_m^6} \right] \quad (6-16)
\end{aligned}$$

and by repeating the reasoning leading up to expression (6-10) the last two terms can be combined to give

$$(D_{2I})^2 = I_0^2 F^4 \left[ \left\langle \left( \sum_{i=1}^N \frac{z_i^2}{r_i^4} \right)^2 \right\rangle - \frac{\pi^2 (\Delta z^3)^2 \sigma^2}{9 r_m^6} \right] \quad (6-17)$$

Examining the first term on the right, one has

$$\begin{aligned}
\left\langle \left( \sum_{i=1}^N \frac{z_i^2}{r_i^4} \right)^2 \right\rangle &= \left\langle \sum_{i=1}^N \frac{z_i^2}{r_i^4} \sum_{i=1}^N \frac{z_i^2}{r_i^4} \right\rangle \\
&= \left\langle \sum_{i=1}^N \frac{z_i^4}{r_i^8} \right\rangle + \left\langle \sum_{i=1}^N \sum_{\substack{k=1 \\ k \neq i}}^N \frac{z_i^2}{r_i^4} \frac{z_k^2}{r_k^4} \right\rangle \\
&= N \left\langle \frac{z_i^4}{r_i^8} \right\rangle + N(N-1) \left\langle \frac{z_i^2}{r_i^4} \frac{z_k^2}{r_k^4} \right\rangle_{i \neq k} \quad (6-18)
\end{aligned}$$

(Terms of this order were previously discarded, but had they been retained at that point, they would have resulted only in terms of even higher order here since the "ones" cancelled in Eq (6-16) prior to squaring.) Looking again at the first term on the right, and following the steps taken between expressions (6-6) and (6-9) gives

$$\begin{aligned}
\left\langle \frac{z_i^4}{r_i^8} \right\rangle &= \frac{\sigma}{N} \int_{z_1}^{z_2} \int_{r_m}^R \int_0^{2\pi} \left( \frac{z_i^4}{r_i^8} \right) r_i' d\theta' dr_i' dz_i' \\
&= \frac{2\pi\sigma}{N} \int_{z_1}^{z_2} z_i'^4 dz_i' \int_{r_m}^R \frac{dr_i'}{r_i'^7} \\
&= \frac{\pi\sigma\Delta z^5}{15N} \left( \frac{1}{r_m^6} - \frac{1}{R^6} \right)
\end{aligned}
\tag{6-19}$$

or, using  $R \gg r_m$ ,

$$\left\langle \frac{z_i^4}{r_i^8} \right\rangle = \frac{\pi\sigma\Delta z^5}{15N r_m^6}
\tag{6-20}$$

In the second term on the right side of Eq (6-18), for  $i \neq k$ , the separate probabilities,  $P_i(r_i, z_i)$  and  $P_k(r_k, z_k)$ , are independent, and the mean of the product equals the product of the means. That is,

$$\begin{aligned}
\left\langle \frac{z_i^2}{r_i^4} \frac{z_k^2}{r_k^4} \right\rangle_{i \neq k} &= \left\langle \frac{z_i^2}{r_i^4} \right\rangle \left\langle \frac{z_k^2}{r_k^4} \right\rangle \\
&= \left\langle \frac{z_i^2}{r_i^4} \right\rangle^2
\end{aligned}
\tag{6-21}$$

or, using Eq (6-10),

$$\left\langle \frac{z_i^2}{r_i^4} \frac{z_k^2}{r_k^4} \right\rangle_{i \neq k} = \frac{\pi^2 \sigma^2 (\Delta z^3)^2}{9N^2 r_m^4}
\tag{6-22}$$

Substituting expressions (6-20) and (6-22) into Eq (6-18) then gives

$$\begin{aligned} \left\langle \left( \sum_{i=1}^N \frac{z_i^2}{r_i^4} \right)^2 \right\rangle &= N \left( \frac{\pi \sigma \Delta z^5}{15 N r_m^6} \right) + (N^2 - N) \left( \frac{\pi^2 \sigma^2 (\Delta z^3)^2}{9 N^2 r_m^4} \right) \\ &= \frac{\pi \sigma \Delta z^5}{15 r_m^6} + \frac{\pi^2 \sigma^2 (\Delta z^3)^2}{9 r_m^4} - \frac{\pi^2 \sigma^2 (\Delta z^3)^2}{9 N r_m^4} \end{aligned} \quad (6-23)$$

Substituting this in turn into Eq (6-17), and cancelling terms, gives

$$\begin{aligned} (D_{2I})^2 &= I_0^2 F^4 \left[ \frac{\pi \sigma \Delta z^5}{15 r_m^6} - \frac{\pi^2 \sigma^2 (\Delta z^3)^2}{9 N r_m^4} \right] \\ &= I_0^2 F^4 \frac{\pi \sigma}{3 r_m^4} \left[ \frac{\Delta z^5}{5 r_m^2} - \frac{\pi \sigma (\Delta z^3)^2}{3 N} \right] \end{aligned} \quad (6-24)$$

or, using expression (6-4) for N,

$$(D_{2I})^2 = I_0^2 F^4 \frac{\pi \sigma}{3 r_m^4} \left[ \frac{\Delta z^5}{5 r_m^2} - \frac{(\Delta z^3)^2}{3 \Delta z R^2} \right] \quad (6-25)$$

As in the previous section, this expression can be simplified and specialized for the particular scenarios. In the first and third scenarios  $\Delta z^5$  reduces to  $(z_2)^5$  and  $(\Delta z^3)^2 / \Delta z$  becomes  $(z_2)^6 / z_2$ , which is also equal to  $(z_2)^5$ . Equation (6-25) is then

$$(D_{2I})^2 = \frac{I_0^2 F^4 \pi \sigma z_2^5}{3 r_m^4} \left[ \frac{1}{5 r_m^2} - \frac{1}{3 R^2} \right]$$

$$\approx \frac{I_0^2 F^4 \pi \sigma z_2^5}{15 r_m^6}$$

(6-26)

which is approximated for  $R \gg r_m$ , and is a general expression for the variance in the intensity changes in scenarios one and three. The r.m.s. deviation,  $D_{2I}$ , in these scenarios is thus

$$D_{2I} = \frac{I_0 F^2}{r_m^3} \sqrt{\frac{\pi \sigma z_2^5}{15}}$$

$$= \frac{I_0 16 M^2 G^2}{c^4 r_m^3} \sqrt{\frac{\pi \sigma z_2^5}{15}}$$

(6-27)

In the second scenario,  $\Delta z^5 = 5z^4 \Delta z$ , and  $(\Delta z^3)^2 = (3z^2 \Delta z)^2 = 9z^4 (\Delta z)^2$ . Equation (6-25) then becomes

$$D_{2I} = \frac{I_0^2 F^4 \pi \sigma z^4 \Delta z}{3 r_m^4} \left[ \frac{1}{r_m^2} - \frac{3}{R^2} \right]$$

$$= \frac{I_0^2 F^4 \pi \sigma z^4 \Delta z}{3 r_m^6}$$

(6-28)

again, having used  $R \gg r_m$ . The r.m.s. intensity change in the second scenario is then

$$D_{2I} = \frac{I_0 F^2 z^2}{r_m^3} \sqrt{\frac{\pi \sigma \Delta z}{3}}$$

$$= \frac{I_0 16 M^2 G^2 z^2}{c^4 r_m^3} \sqrt{\frac{\pi \sigma \Delta z}{3}}$$

(6-29)

### Numerical Evaluation of Intensity Effects

Using appropriate distributions of deflecting masses, expressions (6-13), (6-14), (6-27), and (6-29) can now be used to give some insight into the gravitational intensity effects expected in each scenario. In the case of deflection by stars of the Milky Way, the largest mean and root mean square deviations in intensity occur for sources at or beyond the far edge of the galaxy, viewed through the galactic plane. The pertinent "worst case" values are  $3 \times 10^{-13}$  pc for  $F_s$ ,  $0.1 \text{ pc}^{-3}$  for  $\sigma_s$ , and  $2 \times 10^4$  pc for  $z_2$ . Using the minimum suitable  $r_m$  of  $1.9 \times 10^{-4}$  (based on this  $z$  and a value of 6 for  $w$  in Eq (5-5)), Eq (6-13) gives the mean, net gravitational intensity change for such sources as  $2 \times 10^{-6}$  times  $I_0$ , the unperturbed intensity itself. This is much less than the level of accuracy associated with intensity distance measurements at such ranges and would be even smaller under less extreme conditions. Since all deviations are positive, the small r.m.s. deviation of  $1.7 \times 10^{-4} I_0$ , from Eq (6-27), indicates that there can be very few instances of large intensity deviations. It appears, therefore, that the net gravitational effect of the stars of the Milky Way is apt to contribute no significant error to any given intensity distance measurement.



In the case of sources viewed through the full diameter of other galaxies,  $\Delta z$  is  $2 \times 10^4$  pc, the worst case (maximum) distance,  $z$ , is  $10^8$  pc, and the smallest suitable  $r_m$  (using  $w = 2.5$  in Eq (5-5)) is  $9 \times 10^{-3}$  pc.  $F_s$  and  $\sigma_s$  are again  $3 \times 10^{-13}$  pc and  $0.1 \text{ pc}^{-3}$ . The mean and r.m.s. changes in intensity, from Eqs (6-14) and (6-29), are  $.075I_0$  and  $.06I_0$ , respectively; values which are somewhat less than the level of accuracy of this scenario.

Looking finally, at the third scenario, that of deflection by whole galaxies, the pertinent "worst case" values are 0.01 pc for  $F_g$ ,  $3 \times 10^{-18} \text{ pc}^{-3}$  for  $\sigma_g$ ,  $4 \times 10^9$  pc for  $z_2$ , and 6325 pc for  $r_m$ , (the minimum suitable value based on a value of one for  $w$  in Eq (5-5)). The mean and r.m.s. deviations for such edge of the universe sources, from Eqs (6-13) and (6-27), are  $0.5I_0$  and  $0.3I_0$ , respectively. Again, the typical net gravitational intensity effect is less than the level of accuracy of values associated with this scenario.

### Discussion of Results

The preceding results require some expansion and further discussion before any final conclusions are drawn. More specific, detailed discussion of the particular scenarios will be made more meaningful, however, if some further comment is first made concerning five items common to each.

First, some further discussion of the quantity  $r_m$  is in order. The variable  $r_m$  is really a rather artificially introduced and evaluated quantity. The results obtained are actually limited mean total effects from which the contributions of any individual effects greater than

some threshold, determined by  $r_m$ , have been excluded. As far as the statistical analysis is concerned, the value of  $r_m$  is arbitrary, and what one would like is to find some value for which the resulting limited mean is negligibly small, while at the same time the probability of there being any deflectors with individual effects large enough to be excluded is also negligibly small.

Increasing  $r_m$  reduces the limited mean to any desired value, but at the expense of the excluded cases becoming less rare. On the other hand, because of the singularity in the intensity expressions and their integrals at  $r = 0$ , one can make the mean total intensity change arbitrarily large by letting  $r_m$  approach zero. (In fact, previous results suggesting a large variance in the case of the stellar deflections within the Milky Way are based essentially on the use of a stellar radius for  $r_m$ , although the actual analytic approach and quantities involved are not the same as in this study.) Such results are due to effectively infinite intensity changes that essentially never happen, however, and their significance in terms of the incorporation of gravity effects into typical intensity distance measurements is not evident. The value of  $r_m$  used in this study is, of course, based only on the particular form of an intermediate expression. It happens, however, to be about the most appropriate value for producing meaningful results.

A second point is that clustering, either of stars or of galaxies, has not been accounted for. In fact, celestial bodies are not uniformly distributed, but oftentimes occur in clusters. This should reduce the average effect somewhat, but for sources viewed through a cluster there should be a much greater likelihood of large gravitational effects.

Third, very large intensity changes are not discounted altogether. They are merely shown to be improbable, and when they do occur it is most likely due to the large individual effects of one or a few nearly aligned deflecting masses. Assuming these masses are luminous, their proximity to the source in photographic plates should suggest that an individual analysis (using Eq (4-33) for example) is warranted. If they are unresolved from the source, (which was shown to be likely in both scenarios of stellar deflections), the error due to the source being misinterpreted might well overshadow the error in distance determinations resulting from gravitational effects.

Fourth, while the typical effect may be small with regards to distance measurement accuracy, the mean effect appears large enough under some conditions in scenarios two and three that if any time variations due to motions of the bodies involved are rapid enough, they should be detectable.

Finally, it should be recalled that the levels of accuracy here associated with each scenario are rough estimates and optimistically chosen. This probably reduces the significance of the calculated intensity changes.

We are now in a position to discuss the three scenarios individually. In the first scenario, to the extent that the excluded cylinder of radius  $r_m$  approximates the paraboloidal segment it contains, (defined by Eq (5-5)) this inner cylinder separates the individual deflectors causing more than about a 2 percent intensity change from those causing less. What has been calculated, then, is roughly the mean total change resulting from the combined effects of all deflectors

which individually cause less than a 2 percent intensity change. That mean total gravitational intensity change for worst case sources at or beyond the far galactic rim is indeed negligibly small, ( $2 \times 10^{-6} I_0$  compared to our significant error threshold of about 1 percent) while at the same time, any larger, excluded contributions are negligibly rare (occurring for about one in every ten thousand observed sources). It can readily be concluded, then, that in any given intensity distance measurement the net gravitational effect of all the stars in the Milky Way is not likely to be significant.

The situation is not so clear in the other scenarios. In the second, wherein deflection by stars in other galaxies is considered, it was shown that when individual deflectors causing more than about a 6 percent (from Eq (4-33)) change in intensity were excluded, the mean change in "worst case" sources due to the remaining deflectors (using Eq (5-3)) was  $.075 I_0$ , which is just below the level of accuracy associated with this scenario. (And the r.m.s. change of  $.06 I_0$  indicates that this mean is fairly representative of typical instances.) In this worst case, however, there is a 50 percent chance of an individual deflector being well enough aligned to cause more than a 6 percent intensity change. One might conclude that gravitational intensity effects are, therefore, frequently important under these worst case conditions.

This is probably not the case, however. It is evident that the largest contributions to the mean total change are due to well aligned deflectors, and that their contributions are overestimated by using Eq (5-3). This means that a mean intensity change of 10 percent would

correctly be associated with all those deflectors outside a smaller excluded cylinder, thereby reducing the probability of there being deflectors in a position to give excluded, large individual changes.

More importantly, however, the conditions under which most resolvable sources in other galaxies are observed are not likely to approach this worst case. In particular, (since resolvable stars are most often observed in the periphery of galaxies viewed obliquely) the portion of the galaxy through which stars are viewed is apt to be much shorter than the galactic diameter, and the density of deflecting stars is likely to be lower in that region. These two factors alone reduce the probable number of deflectors causing more than a 6 percent intensity change by a couple orders of magnitude. One can again conclude, then, that at least throughout the majority of conditions under which stars are viewed through other galaxies, gravitational intensity effects remain negligible in terms of their impact on intensity distance measurement.

In the last scenario, in which the effect of entire galaxies acting on a source is considered, the mean intensity change under worst case conditions was shown to be  $.5I_0$ , with an r.m.s. deviation of  $.3I_0$ , which is again somewhat less than the level that would impact distance measurements. However, it was earlier shown that in every such worst case there are apt to be one or two deflectors in a position to individually cause more than a 17 percent intensity change. Here, the possible available reduction of  $r_m$ , as discussed in the previous scenario, would still leave a significant probability of there being deflectors causing notably large intensity changes. In addition, there is no known interfering matter uniquely associated with the worst case conditions to make

it unlikely that sources would be observed at such ranges, and furthermore, the number of sources at a given distance is proportional to the square of the distance, placing many sources at great distances. Well defined sources, however, are apt to be considerably less distant, lowering the probability of large individual deflector effects quite a bit, and it is, therefore, unlikely that many galactic distance determinations have been grossly in error due to gravitational effects. On the other hand, typical effects on the order of the intensity itself could contribute to the uncertainty that exists in characterizing galactic sources. It might well be appropriate to eliminate most gravitational errors in this scenario (even though other inaccuracies are apt to be just as large). Large total effects have been shown to be most likely due to large individual effects, and these could be corrected for, to any desired degree of accuracy, by using expression (4-33) to individually analyze the effects of any deflectors appearing within some selected angular separation from the source (approximating the paraboloid previously discussed, by a cone).

It might also be noted that if galactic coronae prove to exist, considerably increasing the mean galactic mass, the typical effect could turn out to be much larger, making such gravitational corrections definitely in order in this scenario.

## VII. Conclusion

The final results of this study show that for deflecting stars within the Milky Way, significant gravitational changes in the intensity of sources are rare enough, and typical changes small enough, that virtually all intensity distance measurements can safely be made without regard to gravitational effects. Under the extreme worst case conditions of deflection by stars in other galaxies, the typical gravitational intensity change might be minimally significant with regards to distance determinations. Under most conditions, however, the effects are again negligibly small. In the case of deflection by whole galaxies, typical gravitational intensity changes may be on the order of the intensity itself. However, due to the great uncertainty in characterizing the absolute magnitude of galaxies, gravitationally induced errors in distance measurements are probably no larger than many other errors, even in this scenario.

In any scenario, large effects are apt to be due to an individual, closely aligned deflecting mass, rather than the net effect of the overall distribution of deflectors. While the final results of this study are statistical, some of the intermediate results could be used in evaluating such large individual effects. If greatest accuracy is desired, carrying out such a program might be warranted in the case of intensity distance determinations of distant galaxies. In the case of stellar deflecting masses, those sufficiently well aligned to individually cause a large intensity change are not likely to be resolved and

distinguished from the source, so that there would be additional errors in the intensity interpretations. Closely aligned bodies which are resolved from the source, however, would thereby flag themselves as being those warranting individual analyses.

Finally, gravitational intensity changes in the cases both of deflection by stars in other galaxies, and of deflection by whole galaxies, are large enough that they should be detectable if any time variations due to motion of the bodies involved occur on a short enough time scale.



## Bibliography

1. A. Einstein. "Lens-like Action of a Star by the Deviation of Light in the Gravitational Field," Science, 84:506 (4 December 1936).
2. F. Zwicky. Physical Review Letters, Series II, 51:290 (1937).
3. F. Zwicky. Physical Review Letters, Series II, 51:679 (1937).
4. J. Barnothy and M. Barnothy. "Galaxies as Gravitational Lenses," Science, 162:348 (18 October 1968).
5. N. Sanitt. "Quasi-stellar Objects and Gravitational Lenses," Nature, 234:199 (26 November 1971).
6. D. Walsh, R. Carswell and R. Weymann. "0957+561A,B: Twin Quasi-stellar Objects or Gravitational Lens?" Nature, 279:381 (31 May 1979).
7. D. Roberts, P. Greenfield and B. Burke. "The Double Quasar 0957+561: A Radio Study at 6 Centimeter Wavelength," Science, 205:894 (31 August 1979).
8. P. Greenfield, D. Roberts, B. Burke. "The Double Quasar 0957+561: Examination of the Gravitational Lens Hypothesis Using the Very Large Array," Science, 208:495 (2 May 1980).
9. P. Young, J. Gunn, J. Kristian, J. Oke, and J. Westphal. "The Double Quasar Q0957+561A,B: Gravitational Lens Image Formed by Galaxy at  $z=0.39$ ," Astrophysical Journal, 241:507 (15 October 1980).
10. A. Haschick, J. Moran, M. Reid, M. Davis, and A. Lilley. "VLBI Observations of Double Quasar 0957+561," Astrophysical Journal Letters, 243:L57 (15 January 1981).
11. P. Young, J. Gunn, J. Kristian, J. Oke, and J. Westphal. "Q0957+561: Detailed Models of the Gravitational Lens Effect," Astrophysical Journal, 244:736 (15 March 1981).
12. R. Cook. "Effect of the Interstellar Gravitational Field on the Apparent Brightness of a Distant Light Source," unpublished.
13. S. Weinberg. Gravitation and Cosmology, Principles and Applications of the General Theory of Relativity, (John Wiley & Sons, 1972).
14. J. Lequeux. Structure and Evolution of Galaxies, (Gordon and Breach Science Publishers, 1969).

15. S. Faber, J. Gallagher. "Masses and Mass-to-Light Ratios of Galaxies," Annual Review of Astronomy and Astrophysics, 17:135 (1979).
16. C. Allen. Astrophysical Quantities, (Athlone Press, University of London, 1955).
17. P. Hodge. "The Extragalactic Distance Scale," Annual Review of Astronomy and Astrophysics, 19:357 (1981).
18. S. Liebes. "Gravitational Lenses," Physical Review, 133:B835 (10 February 1964).
19. A. Labeyrie. "Stellar Interferometry Methods," Annual Review of Astronomy and Astrophysics, 16:77 (1978).

## Appendix A

### Summary of Pertinent Calculations from General Relativity

This appendix shows the basic calculations of general relativity theory leading to the results used as a starting point in the main report. Schwarzschild, in 1916, found the exact solution to the gravitational field equations external to a spherically symmetric mass distribution, and the following calculations are usually based on that exact solution (although the resulting trajectory equation must still be solved by approximation). In this appendix, however, a perturbation approach is taken throughout, although the specific case addressed is the spherically symmetric point mass. In the weak field regime where this approach is valid (and this regime includes most physically realizable conditions), the results are the same within the order of approximation used. For details of the calculations using the Schwarzschild solution see, for example, Introduction to General Relativity by Adler, Bazin and Schiffer (McGraw-Hill, 1965).

### Conventions, Postulates, and Assumptions

1. The following conventions and definitions are employed in the tensor analysis:

- a. Roman indices range from one to three
- b. Greek indices range from zero to three, with the zero index belonging to the time coordinate.
- c.  $T^i_{j|p}$  denotes partial differentiation of the tensor  $T^i_j$  with respect to the  $p^{\text{th}}$  coordinate. (A double bar is used to denote

covariant differentiation.)

d. The substitution tensor in any form ( $\delta_{ij}$ ,  $\delta^{ij}$  or  $\delta_j^i$ ) has the value one when  $i$  equals  $j$ , and zero otherwise.

e. The appearance of a double index, once covariant and once contravariant, in a single tensor term or tensor product implies summation over the range of that index (e.g.,  $X_i^{ai} = X_1^{a1} + X_2^{a2} + X_3^{a3}$ ). Summation is not implied when:

- (1) The indices are both covariant or contravariant.
- (2) Specific numerical values are expressed for the indices (e.g.,  $P_2^2$ ).
- (3) The indices are written parenthetically (e.g.,  $A \begin{smallmatrix} (i) \\ (i) \end{smallmatrix}$ ).

f. The curvature of a Riemann space is described by its (covariant) metric tensor  $g_{\alpha\beta}$  or, equivalently, by its inverse, the contravariant metric tensor  $g^{\alpha\beta}$ .

g. The Christoffel symbol of the second kind,  $\left\{ \begin{smallmatrix} \alpha \\ \beta \gamma \end{smallmatrix} \right\}$ , is defined by

$$\left\{ \begin{smallmatrix} \alpha \\ \beta \gamma \end{smallmatrix} \right\} \equiv \frac{1}{2} g^{\alpha\tau} (g_{\beta\tau|\gamma} + g_{\tau\gamma|\beta} - g_{\tau\alpha|\gamma}) \quad (A-1)$$

2. The following are postulates of general relativity:

a. Gravitational effects are accounted for by the curvature of space-time. Thus, the gravitational field equations are in fact equations for the metric tensor  $g_{\alpha\beta}$ .

b. Motion of a free particle in 4-space is along a geodesic (the Riemannian equivalent to a Euclidean straight line). A free particle is one upon which the only forces that act are those arising

from the choice of coordinate system (i.e., centrifugal, coriolis, gravitational).

c. The trajectories of light rays are null geodesics.

That is, along a ray path the 4-space path element vanishes, or

$$(ds)^2 = 0 = g_{\alpha\beta} dx^\alpha dx^\beta \quad (\text{A-2})$$

3. The following assumptions and approximations are made:

a. The self-source action of gravitational fields is neglected.

b. A time independent situation is considered in which the actual metric tensor is given by a constant perturbation,  $\epsilon\gamma_{\alpha\beta}$ , to the constant and uniform Lorentz metric,

$$g_{\alpha\beta}^{(L)} = g^{(L)\alpha\beta} = \begin{pmatrix} 1 & 0 & 0 & 0 \\ 0 & -1 & 0 & 0 \\ 0 & 0 & -1 & 0 \\ 0 & 0 & 0 & -1 \end{pmatrix} \quad (\text{A-3})$$

where  $\gamma_{\alpha\beta}$  vanishes at infinity and only terms to first order in  $\epsilon$  are retained in calculations.

c. The perturbation is assumed to be diagonal, the justification being that such a form works.

d. When spherical symmetry exists one can find an isotropic coordinate system in which  $g_{11} = g_{22} = g_{33}$  so that in this case

$$\gamma_{11} = \gamma_{22} = \gamma_{33} \equiv \gamma_{zz} \quad (\text{no sum}).$$

Thus

$$g_{\alpha\beta} = g_{\alpha\beta}^{(L)} + \epsilon \gamma_{\alpha\beta} = \begin{pmatrix} 1 + \epsilon \gamma_{00} & 0 & 0 & 0 \\ 0 & -1 + \epsilon \gamma_{zz} & 0 & 0 \\ 0 & 0 & -1 + \epsilon \gamma_{zz} & 0 \\ 0 & 0 & 0 & -1 + \epsilon \gamma_{zz} \end{pmatrix} \quad (\text{A-4})$$

and, to order  $\epsilon$ ,

$$g^{\alpha\beta} = g^{\alpha\beta (L)} + \epsilon \gamma^{\alpha\beta} = \begin{pmatrix} 1 - \epsilon \gamma_{00} & 0 & 0 & 0 \\ 0 & -1 - \epsilon \gamma_{zz} & 0 & 0 \\ 0 & 0 & -1 - \epsilon \gamma_{zz} & 0 \\ 0 & 0 & 0 & -1 - \epsilon \gamma_{zz} \end{pmatrix} \quad (\text{A-5})$$

In such a system, the coordinate velocity of light at a point is the same in every direction, but varies with the radial coordinate. This isotropic radial coordinate ( $\rho$  in this appendix) is not necessarily the same as the flat space radial distance coordinate ( $r$  in this appendix), but is some function of it.

#### Derivation of Euler's Equations

Since the trajectories of light rays are geodesics, it is useful in determining ray paths to have the geodesic differential equation. This is obtained from the Euler-Lagrange equations of the system, which are themselves the equations of motion of the system. The Euler equations are derived from the variational problem, which in this case is

$$\delta \int_{P_1}^{P_2} \sqrt{g_{\alpha\beta} \frac{dx^\alpha}{dq} \frac{dx^\beta}{dq}} dq = 0$$

(A-6)

where  $p_1$  and  $p_2$  are endpoints and  $q$  is a parameter which varies along the curve (other than path length since  $ds = 0$  along the null geodesic light trajectories). This problem is the mathematical specification that the integral be minimized along the actual path (that is, its variation between "adjacent" possible paths will be zero along the true path).

An equivalent problem is

$$\delta \int_{P_1}^{P_2} g_{\alpha\beta} \frac{dx^\alpha}{dq} \frac{dx^\beta}{dq} dq = 0$$

(A-7)

or

$$\delta I = \delta \int_{P_1}^{P_2} \Psi \left( x^\alpha, \frac{dx^\alpha}{dq} \right) dq = 0$$

(A-8)

where  $I$  represents the entire integral in (A-7) and  $\Psi$  the integrand alone. Following standard procedures of the calculus of variations one considers a family of possible curves, all joining  $p_1$  and  $p_2$ , and close to the true path. Using the simple  $\delta$  notation, one then considers the variations of the integral when evaluated along different possible curves, and has

$$\delta I = \int_{P_1}^{P_2} \left[ \frac{\partial \Psi}{\partial x^\alpha} \delta x^\alpha + \frac{\partial \Psi}{\partial \left( \frac{dx^\alpha}{dq} \right)} \delta \left( \frac{dx^\alpha}{dq} \right) \right] dq$$

(A-9)

or

$$\delta I = \int_{p_1}^{p_2} \left[ \frac{\partial \Psi}{\partial x^{\alpha}} \delta x^{\alpha} + \frac{\partial \Psi}{\partial \left( \frac{dx^{\alpha}}{dq} \right)} \frac{d}{dq} (\delta x^{\alpha}) \right] dq \quad (\text{A-10})$$

Integrating the second term by parts gives

$$\delta I = \int_{p_1}^{p_2} \frac{\partial \Psi}{\partial x^{\alpha}} \delta x^{\alpha} dq + \left[ \frac{\partial \Psi}{\partial \left( \frac{dx^{\alpha}}{dq} \right)} \delta x^{\alpha} \right]_{p_1}^{p_2} - \int_{p_1}^{p_2} \delta x^{\alpha} \frac{d}{dq} \left( \frac{\partial \Psi}{\partial \left( \frac{dx^{\alpha}}{dq} \right)} \right) dq \quad (\text{A-11})$$

Since all curves connect  $p_1$  and  $p_2$ , there is no variation of  $x^{\gamma}$  at the endpoints, thus  $\delta x^{\gamma} = 0$  at  $p_1$  and  $p_2$  and the middle term vanishes in (A-11) leaving

$$\delta I = 0 = \int_{p_1}^{p_2} \left[ \frac{\partial \Psi}{\partial x^{\alpha}} - \frac{d}{dq} \left( \frac{\partial \Psi}{\partial \left( \frac{dx^{\alpha}}{dq} \right)} \right) \right] \delta x^{\alpha} dq \quad (\text{A-12})$$

Since  $\delta x^{\gamma}$  is in general not zero, Eq (A-12) can be assured by requiring the expression in brackets to be identically zero. Thus,

$$\frac{\partial \Psi}{\partial x^{\alpha}} - \frac{d}{dq} \left( \frac{\partial \Psi}{\partial \left( \frac{dx^{\alpha}}{dq} \right)} \right) = 0 \quad (\text{A-13})$$

which, in general form, are the Euler-Lagrange equations for the system.

#### Reduction to the Standard Geodesic Equations

The Euler equations together describe extremal paths, and using our  $\Psi$  they can be reduced to the geodesic equations in standard form. Using tensor notation and the fact that the derivatives,  $\frac{dx^{\gamma}}{dq}$ , are not explicit functions of  $x^{\gamma}$ ,



$$\frac{\partial \Psi}{\partial x^{\alpha}} = \Psi_{|\alpha} = g_{\alpha\beta|\gamma} \frac{dx^{\alpha}}{dq} \frac{dx^{\beta}}{dq} \quad (\text{A-14})$$

Also, since  $g_{\alpha\beta}$  is not an explicit function of  $\frac{dx^{\gamma}}{dq}$ ,

$$\begin{aligned} \frac{\partial \Psi}{\partial \left(\frac{dx^{\alpha}}{dq}\right)} &= g_{\alpha\beta} \left[ \frac{\partial \left(\frac{dx^{\alpha}}{dq}\right)}{\partial \left(\frac{dx^{\alpha}}{dq}\right)} \frac{dx^{\beta}}{dq} + \frac{dx^{\alpha}}{dq} \frac{\partial \left(\frac{dx^{\beta}}{dq}\right)}{\partial \left(\frac{dx^{\alpha}}{dq}\right)} \right] \\ &= g_{\alpha\beta} \left[ \delta_{\alpha}^{\beta} \frac{dx^{\beta}}{dq} + \frac{dx^{\alpha}}{dq} \delta_{\alpha}^{\beta} \right] \\ &= g_{\alpha\beta} \frac{dx^{\beta}}{dq} + g_{\alpha\alpha} \frac{dx^{\alpha}}{dq} \\ &= 2 g_{\alpha\beta} \frac{dx^{\beta}}{dq} \end{aligned}$$

(A-15)

since  $g_{\alpha\beta}$  is symmetric and the choice of summation indices is immaterial.

Then

$$\frac{d}{dq} \left( \frac{\partial \Psi}{\partial \left(\frac{dx^{\alpha}}{dq}\right)} \right) = 2 g_{\alpha\beta} \frac{d^2 x^{\beta}}{dq^2} + 2 g_{\alpha\beta|\gamma} \frac{dx^{\alpha}}{dq} \frac{dx^{\beta}}{dq} \quad (\text{A-16})$$

But

$$g_{\alpha\beta|\gamma} \frac{dx^{\alpha}}{dq} \frac{dx^{\beta}}{dq} = g_{\alpha\beta|\gamma} \frac{dx^{\beta}}{dq} \frac{dx^{\alpha}}{dq} \quad (\text{A-17})$$

simply by switching summation indices. Equation (A-16) can thus be written

$$\frac{d}{dq} \left( \frac{\partial \Psi}{\partial \left( \frac{dx^\alpha}{dq} \right)} \right) = 2g_{\alpha\beta} \frac{d^2 x^\beta}{dq^2} + g_{\alpha\gamma|\eta} \frac{dx^\eta}{dq} \frac{dx^\beta}{dq} + g_{\alpha\eta|\beta} \frac{dx^\beta}{dq} \frac{dx^\eta}{dq} \quad (\text{A-18})$$

Changing the summation index  $\alpha$  in Eq (A-14) to  $\eta$ , substituting Eqs (A-14) and (A-18) into Eq (A-13), and multiplying by  $(-1/2)$  gives

$$g_{\alpha\beta} \frac{d^2 x^\beta}{dq^2} + \frac{1}{2} \left[ g_{\alpha\gamma|\eta} \frac{dx^\eta}{dq} \frac{dx^\beta}{dq} + g_{\alpha\eta|\beta} \frac{dx^\beta}{dq} \frac{dx^\eta}{dq} - g_{\eta\beta|\alpha} \frac{dx^\beta}{dq} \frac{dx^\eta}{dq} \right] = 0 \quad (\text{A-19})$$

When multiplied by  $g^{\nu\gamma}$ , these equations can be written

$$\frac{d^2 x^\nu}{dq^2} + \left\{ \begin{matrix} \nu \\ \eta\beta \end{matrix} \right\} \frac{dx^\beta}{dq} \frac{dx^\eta}{dq} = 0 \quad (\text{A-20})$$

the standard equations for a geodesic.

Having established the equivalence of the geodesic equations with Euler's equations, it can be seen that a quick way to calculate Christoffel symbols for a system with known equations of motion is to equate the corresponding terms in the Euler and geodesic equations.

#### Linearization of the Field Equations

For present purposes, the metric tensor must be known in order to use either the geodesic or the Euler equations. To determine the metric, the field equations must be solved. The empty space gravitational field equations for the metric tensor, chosen by Einstein, are equivalent to  $R_{\eta\lambda} = 0$ , where  $R_{\eta\lambda}$  is the contracted Riemann-Christoffel

tensor of the second kind,  $R_{\gamma\alpha\lambda}^{\alpha}$ .

From its definition, the field equations may be written

$$0 = \left\{ \begin{matrix} \beta \\ \beta\gamma \end{matrix} \right\}_{|\lambda} - \left\{ \begin{matrix} \beta \\ \lambda\gamma \end{matrix} \right\}_{|\beta} + \left\{ \begin{matrix} \beta \\ \gamma\lambda \end{matrix} \right\} \left\{ \begin{matrix} \gamma \\ \beta\eta \end{matrix} \right\} + \left\{ \begin{matrix} \beta \\ \gamma\beta \end{matrix} \right\} \left\{ \begin{matrix} \gamma \\ \lambda\eta \end{matrix} \right\} \quad (\text{A-21})$$

To solve these equations, the perturbed Lorentz form is assumed for the metric and terms of order  $\epsilon^2$  or higher are discarded. From Eqs (A-1), (A-4) and (A-5), the Christoffel symbols may be written

$$\left\{ \begin{matrix} \alpha \\ \beta\gamma \end{matrix} \right\} = \frac{1}{2} \left[ g^{(L)\alpha\lambda} + \epsilon \gamma^{\lambda\alpha} \right] \left[ g^{(L)}_{\gamma\lambda|\beta} + \epsilon \delta^{\lambda}_{\gamma|\beta} + g^{(L)}_{\delta\beta|\lambda} \right. \\ \left. + \epsilon \delta^{\lambda}_{\delta\beta|\lambda} - g^{(L)}_{\delta\beta|\lambda} - \epsilon \delta^{\lambda}_{\beta\lambda|\delta} \right] \quad (\text{A-22})$$

By the constancy and uniformity of the Lorentz metric,

$$g^{(L)}_{\lambda\beta|\delta} = g^{(L)\lambda\beta}_{|\delta} = 0 \quad (\text{A-23})$$

Thus, to order  $\epsilon$ , the Christoffel symbols reduce to

$$\left\{ \begin{matrix} \alpha \\ \beta\gamma \end{matrix} \right\} = \frac{\epsilon}{2} g^{(L)\alpha\lambda} \left[ \delta^{\lambda}_{\gamma|\beta} + \delta^{\lambda}_{\delta\beta|\lambda} - \delta^{\lambda}_{\beta\lambda|\delta} \right] \quad (\text{A-24})$$

The Christoffel symbols themselves are, therefore, of order  $\epsilon$  and the last two terms in (A-21), being of order  $\epsilon^2$ , are dropped.

Using Eqs (A-23) and (A-24), the first term in (A-21) can be written

$$\left\{ \begin{matrix} \beta \\ \beta \gamma \end{matrix} \right\}_{|\lambda} = \frac{\epsilon}{2} g^{(L)\beta\mu} \left( \gamma_{\gamma\mu|\beta|\lambda} + \gamma_{\mu\beta|\gamma|\lambda} - \gamma_{\beta\gamma|\mu|\lambda} \right) \quad (\text{A-25})$$

Here, by interchanging indices of the symmetric tensors  $g^{(L)\alpha\beta}$  and  $\gamma_{\alpha\beta}$  in the third term, and then interchanging the summation indices, the first and third terms cancel, leaving

$$\left\{ \begin{matrix} \beta \\ \beta \gamma \end{matrix} \right\}_{|\lambda} = \frac{\epsilon}{2} g^{(L)\beta\mu} \gamma_{\mu\beta|\gamma|\lambda} \quad (\text{A-26})$$

Again using Eqs (A-24) and (A-23), the second term in (A-21) becomes

$$-\left\{ \begin{matrix} \beta \\ \lambda \gamma \end{matrix} \right\}_{|\beta} = -\frac{\epsilon}{2} g^{(L)\beta\mu} \left( \gamma_{\gamma\mu|\lambda|\beta} + \gamma_{\mu\lambda|\gamma|\beta} - \gamma_{\lambda\gamma|\mu|\beta} \right) \quad (\text{A-27})$$

Using (A-26) and (A-27), the field Eqs (A-21) thus reduce to the linearized form

$$0 = g^{(L)\beta\mu} \left[ \gamma_{\mu\beta|\gamma|\lambda} - \gamma_{\gamma\mu|\lambda|\beta} - \gamma_{\mu\lambda|\gamma|\beta} + \gamma_{\lambda\gamma|\mu|\beta} \right] \quad (\text{A-28})$$

#### Relation Between $\gamma_{00}$ and $\gamma_{zz}$

Looking at the Eq (A-28) for  $\gamma = \lambda = 0$ , the first three terms vanish by time independence of  $\gamma_{\alpha\beta}$ . Those terms in the remaining sum for which  $\mu = 0$  or  $\beta = 0$  also vanish by time independence, leaving

$$\begin{aligned} 0 &= g^{(L)ij} \gamma_{00|ij} \\ &= -\delta^{ij} \gamma_{00|ij} \end{aligned} \quad (\text{A-29})$$

or, in vector notation,

$$\nabla^2 \gamma_{00} = 0 \quad (\text{A-30})$$

In the Eqs (A-28) for  $\lambda = \eta = i \neq 0$ , the two middle terms are equal by the symmetry of  $\gamma_{\alpha\beta}$ . Thus

$$0 = g^{(L)\beta\mu} \left[ \gamma_{\mu\beta|(i)(i)} - 2\gamma_{(i)\mu|(i)\beta} + \gamma_{(i)(i)|\mu\beta} \right] \quad (\text{A-31})$$

Since  $g^{(L)\alpha\beta}$  is diagonal, many zero valued terms can be dropped from these equations. Using  $g^{(L)00} = 1$  and  $g^{(L)ik} = -\delta^{ik}$ , and distributing the Lorentz metric, leaves

$$\begin{aligned} 0 &= g^{(L)00} \gamma_{00|(i)(i)} - 2g^{(L)00} \gamma_{(i)0|(i)0} + g^{(L)00} \gamma_{(i)(i)|00} \\ &\quad - \delta^{kl} \gamma_{kl|(i)(i)} + 2\delta^{kl} \gamma_{(i)k|(i)l} - \delta^{kl} \gamma_{(i)(i)|kl} \\ &= \gamma_{00|(i)(i)} - \delta^{kl} \gamma_{kl|(i)(i)} + 2\delta^{kl} \gamma_{(i)k|(i)l} - \delta^{kl} \gamma_{(i)(i)|kl} \end{aligned} \quad (\text{A-32})$$

where the second and third terms vanished by time independence. Now  $\gamma_{kl} = \delta_{kl} \gamma_{zz}$  and since  $\delta_{kl}$  is uniform and constant it commutes with the operation of partial differentiation, so that

$$\gamma_{kl|\beta|\lambda} = \delta_{kl} \gamma_{zz|\beta|\lambda} \quad (\text{A-33})$$

Using this, Eqs (A-32) can be written

$$\begin{aligned}
 0 &= \gamma_{00|(i)(i)} - \delta^{kl} \delta_{kl} \gamma_{zz|(i)(i)} + 2 \delta^{kl} \delta_{(i)k} \delta'_{zz|(i)l} - \delta^{kl} \delta_{(i)l} \delta'_{zz|(i)k} \\
 &= \gamma_{00|(i)(i)} - 3 \gamma_{zz|(i)(i)} + 2 \gamma'_{zz|(i)(i)} - \delta^{kl} \gamma'_{zz|kl} \\
 &= \gamma'_{00|(i)(i)} - \gamma'_{zz|(i)(i)} - \delta^{kl} \gamma'_{zz|kl}
 \end{aligned} \tag{A-34}$$

Adding Eq (A-34) for  $i = 1, 2$  and  $3$  gives

$$0 = \delta^{kl} \gamma'_{00|kl} - \delta^{kl} \gamma'_{zz|kl} - 3 \delta^{kl} \gamma'_{zz|kl} \tag{A-35}$$

or, using (A-29),

$$0 = \delta^{kl} \gamma'_{zz|kl} \tag{A-36}$$

Using this result in Eqs (A-34), and combining terms, gives

$$0 = (\gamma'_{00} - \gamma'_{zz})_{|(i)(i)} \tag{A-37}$$

These equations imply that  $(\gamma'_{00} - \gamma'_{zz})$  is linear. Since  $\gamma_{\alpha\beta}$  vanishes at infinity,  $(\gamma'_{00} - \gamma'_{zz})$  must then be zero everywhere. Thus

$$\gamma'_{00} = \gamma'_{zz} \tag{A-38}$$

### Calculation of $\gamma_{00}$

The perturbation  $\epsilon\gamma_{00}$  is determined by correspondence with classical laws of motion in the limit of a weak perturbation (small  $\epsilon$ ) and velocities much less than  $c$  (small  $\beta = \frac{v}{c}$ ). Calculations carry only terms to first order in  $\epsilon$  or  $\beta$ . We consider the motion of a free particle and repeat here the equations of its geodesic path derived earlier.

$$\frac{d^2 x^\alpha}{ds^2} + \left\{ \begin{matrix} \alpha \\ \gamma \ \tau \end{matrix} \right\} \frac{dx^\gamma}{ds} \frac{dx^\tau}{ds} = 0 \quad (\text{A-20})$$

The first term can be written

$$\frac{d^2 x^\alpha}{ds^2} = \frac{d^2 x^\alpha}{dt^2} \left( \frac{dt}{ds} \right)^2 \quad (\text{A-39})$$

and in the second term

$$\frac{dx^\gamma}{ds} \frac{dx^\tau}{ds} = \frac{dx^\gamma}{dt} \frac{dx^\tau}{dt} \left( \frac{dt}{ds} \right)^2 \quad (\text{A-40})$$

Substituting these expressions into (A-20) and dividing through by

$c^2 \left( \frac{dt}{ds} \right)^2$  gives

$$\frac{d^2 x^\alpha}{c^2 dt^2} + \left\{ \begin{matrix} \alpha \\ \gamma \ \tau \end{matrix} \right\} \frac{dx^\gamma}{cdt} \frac{dx^\tau}{cdt} = 0 \quad (\text{A-41})$$

The Christoffel symbols were shown previously (Eq (A-24)) to be of order  $\epsilon$ , and the derivatives in the second term of (A-41) equal  $c$  if

their index is zero, and a component of the velocity (of order  $\beta$ ) otherwise. Discarding terms of order  $\epsilon\beta$  and  $\epsilon\beta^2$  in Eq (A-41) leaves only the  $\eta = \tau = 0$  terms. Multiplying through by  $c^2$  gives

$$\frac{d^2 x^\alpha}{dt^2} + c^2 \left\{ \begin{matrix} \alpha \\ 00 \end{matrix} \right\} = 0 \quad (\text{A-42})$$

Using Eq (A-24) and the result of time independence that  $\gamma_{\alpha\beta|0} = 0$ , the pertinent Christoffel symbols can, to order  $\epsilon$ , be written

$$\left\{ \begin{matrix} \alpha \\ 00 \end{matrix} \right\} = -\frac{\epsilon}{2} g^{\alpha\lambda} \gamma_{00|\lambda} \quad (\text{A-43})$$

For  $\alpha = 0$  this becomes

$$\left\{ \begin{matrix} 0 \\ 00 \end{matrix} \right\} = -\frac{\epsilon}{2} g^{0\lambda} \gamma_{00|\lambda} = 0 \quad (\text{A-44})$$

since the only non-zero  $g^{0\lambda}$  is  $g^{00}$ , and  $\gamma_{00|0}$  is zero by time independence. The  $\alpha = 0$  Eq (A-42) thus gives

$$\frac{d^2 x^0}{dt^2} = \frac{d^2(ct)}{dt^2} = 0 \quad (\text{A-45})$$

as it should.

For  $\alpha = i \neq 0$ , the diagonality of  $g^{(L)\alpha\beta}$  leads to

$$\begin{aligned} \left\{ \begin{matrix} i \\ 00 \end{matrix} \right\} &= -\frac{\epsilon}{2} g^{(L)ij} \gamma_{00|j} \\ &= +\frac{\epsilon}{2} \delta^{ij} \gamma_{00|j} \end{aligned} \quad (\text{A-46})$$



Thus

$$\frac{d^2 x^i}{dt^2} + c^2 \frac{\epsilon}{2} \delta^{ij} \gamma_{00lj} = 0 \quad (\text{A-47})$$

or, in vector form,

$$\frac{d^2 \vec{x}}{dt^2} = \frac{c^2 \epsilon}{2} \nabla \gamma_{00} \quad (\text{A-48})$$

This result must correspond with Newton's equation of motion of a mass  $M$  in the field of a force,  $\vec{F}$ , derived from a scalar potential,  $\Phi$ ,

$$\frac{d^2 \vec{x}}{dt^2} = \frac{\vec{F}}{M} = -\nabla \Phi \quad (\text{A-49})$$

Therefore

$$\epsilon \gamma_{00} = \frac{\partial \Phi}{c^2} = \epsilon \gamma_{zz} \quad (\text{A-50})$$

and Eq (A-30) is now seen to be the classical gravitational potential field equation.

The final results are thus

$$g_{\mu\nu} = \begin{pmatrix} 1 + \frac{2\Phi}{c^2} & 0 & 0 & 0 \\ 0 & -1 + \frac{2\Phi}{c^2} & 0 & 0 \\ 0 & 0 & -1 + \frac{2\Phi}{c^2} & 0 \\ 0 & 0 & 0 & -1 + \frac{2\Phi}{c^2} \end{pmatrix} \quad (\text{A-51})$$

and

$$g^{\alpha\beta} = \begin{pmatrix} 1 - \frac{2\Phi}{c^2} & 0 & 0 & 0 \\ 0 & -1 - \frac{2\Phi}{c^2} & 0 & 0 \\ 0 & 0 & -1 - \frac{2\Phi}{c^2} & 0 \\ 0 & 0 & 0 & -1 - \frac{2\Phi}{c^2} \end{pmatrix} \quad (\text{A-52})$$

Where for a mass M at the origin

$$\Phi(r) = -\frac{MG}{r} \quad (\text{A-53})$$

G being the universal gravitational constant and r being the radial distance coordinate. Strictly speaking, the isotropic radial coordinate,  $\rho$ , was used in this appendix, but as is shown in the beginning of Appendix B,  $\rho$  and r are interchangeable in these expressions, to the level of approximation carried (first order in  $\frac{MG}{c^2}$ ) in the weak field region of concern ( $r \gg \frac{MG}{c^2}$ ).

AD-A127 514

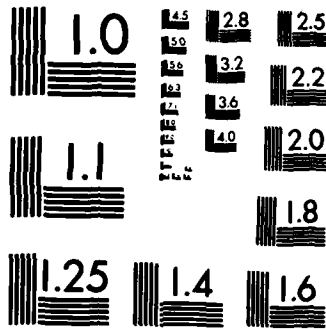
THE NET EFFECT OF MANY GRAVITATIONAL FIELDS ON THE  
INTENSITY OF CELESTIAL (U) AIR FORCE INST OF TECH  
WRIGHT-PATTERSON AFB OH SCHOOL OF ENGI... G E CIPPERLY  
DEC 82 AFIT/GEP/PH/82D-4 F/G 3/2

2/2

UNCLASSIFIED

NL





MICROCOPY RESOLUTION TEST CHART  
NATIONAL BUREAU OF STANDARDS-1963-A

Appendix B

4-Space Calculation of the Deflection of Light Rays

As stated in Appendix A, the trajectory of a light ray is a solution to the variational problem

$$\delta \int_{P_1}^{P_2} \sqrt{g_{\alpha\beta} \frac{dx^\alpha}{dq} \frac{dx^\beta}{dq}} dq = 0 \quad (\text{B-1})$$

or, equivalently,

$$\delta \int_{P_1}^{P_2} g_{\alpha\beta} \frac{dx^\alpha}{dq} \frac{dx^\beta}{dq} dq = 0 \quad (\text{B-2})$$

where  $q$  is a parameter along the path (other than the path length,  $s$ , since  $ds = 0$  along a null geodesic).

In considering rays in the field of a point mass, it is most convenient to use spherical coordinates. Using the weak field metric tensor determined in Appendix A, and the simplifying notation  $F = \frac{4MG}{c^2}$ , the path element in isotropic spherical coordinates is

$$\begin{aligned} ds^2 = 0 &= g_{\alpha\beta} \frac{dx^\alpha}{dq} \frac{dx^\beta}{dq} \\ &= \left(1 - \frac{F}{2\rho}\right) c^2 dt^2 - \left(1 + \frac{F}{2\rho}\right) \left[ \rho^2 d\theta^2 + \rho^2 \sin^2\theta d\phi^2 \right] \end{aligned} \quad (\text{B-3})$$

It will be expedient, however, to forego using isotropic coordinates and find the simpler, equivalent metric of the form

$$ds^2 = 0 = A(r)c^2 dt^2 - B(r)dr^2 - r^2 d\theta^2 - r^2 \sin^2 \theta d\phi^2 \quad (\text{B-4})$$

where  $r$  is the radial distance coordinate.

Equating the angular coefficients of (B-3) and (B-4) gives

$$\begin{aligned} -r^2 &= -\left(1 + \frac{F}{2\rho}\right)\rho^2 \\ &= -\rho^2 - \frac{F\rho}{2} \end{aligned} \quad (\text{B-5})$$

and solving this quadratic for  $\rho(r)$  gives

$$\rho(r) = -\frac{F}{4} \pm r\sqrt{\frac{F^2}{16r^2} + 1} \quad (\text{B-6})$$

or, to first order in  $F$ ,

$$\rho(r) = r\left(1 - \frac{F}{4r}\right) \quad (\text{B-7})$$

where the plus sign was chosen in (B-6) for closest correspondence between  $r$  and  $\rho$ . Then by correspondence of coefficients, substitution, and dropping second order terms in  $F$ ,

$$\begin{aligned} A(r) &= \left(1 - \frac{F}{2\rho(r)}\right) \\ &= 1 - \frac{F}{2r\left(1 - \frac{F}{4r}\right)} \\ &\approx 1 - \frac{F}{2r} \end{aligned} \quad (\text{B-8})$$

and

$$\begin{aligned} B(r) &= \left(1 + \frac{F}{2\rho(r)}\right) \\ &= 1 + \frac{F}{2r} \end{aligned} \quad (\text{B-9})$$

Thus, to our order of approximation, the metric tensor time and radial components appear unchanged, and the angular components revert to the (-1) values of the unperturbed Lorentz metric. This metric agrees with the Schwarzschild metric in non-isotropic coordinates, approximated for small F.

The variational problem (B-2) is now

$$\delta \int_{P_1}^{P_2} \left[ \left(1 - \frac{F}{2r}\right) c^2 \left(\frac{dt}{dq}\right)^2 - \left(1 + \frac{F}{2r}\right) \left(\frac{dr}{dq}\right)^2 - r^2 \left(\frac{d\theta}{dq}\right)^2 - r^2 \sin^2 \theta \left(\frac{d\phi}{dq}\right)^2 \right] dq = 0 \quad (\text{B-10})$$

Using Eq (A-13), the Euler equations are:

$$\text{for } t, \quad \frac{d}{dq} \left[ \left(1 - \frac{F}{2r}\right) \frac{dt}{dq} \right] = 0 \quad (\text{B-11})$$

$$\text{for } \theta, \quad \frac{d}{dq} \left[ -2r^2 \frac{d\theta}{dq} \right] = -2r^2 \sin \theta \cos \theta \left(\frac{d\phi}{dq}\right)^2 \quad (\text{B-12})$$

$$\text{for } \phi, \quad \frac{d}{dq} \left[ r^2 \sin^2 \theta \frac{d\phi}{dq} \right] = 0 \quad (\text{B-13})$$

The Euler equation for r may be replaced by the simpler equation obtained by dividing the null line element by  $(dq)^2$ . The fourth equation in the system is then

$$\left(\frac{ds}{dq}\right)^2 = 0 = \left(1 - \frac{F}{2r}\right) c^2 \left(\frac{dt}{dq}\right)^2 - \left(1 + \frac{F}{2r}\right) \left(\frac{dr}{dq}\right)^2 - r^2 \left(\frac{d\theta}{dq}\right)^2 - r^2 \sin^2 \theta \left(\frac{d\phi}{dq}\right)^2 \quad (\text{B-14})$$

It is evident that by proper alignment of the axes, one can establish

$$\left. \begin{aligned} \theta &= \frac{\pi}{2} \\ \sin \theta &= 1 \\ \cos \theta &= 0 \\ \frac{d\theta}{dq} &= 0 \end{aligned} \right\} \text{(B-15)}$$

for all  $q$ , causing Eq (B-12) to disappear. That is to say, the trajectory and center of mass lie within a plane in three space, as expected. Using (B-15), Eq (B-13) can be integrated to give

$$r^2 \frac{d\phi}{dq} = A \quad \text{(B-16)}$$

Similarly, Eq (B-11) yields

$$\left(1 - \frac{F}{2r}\right) \frac{dt}{dq} = B \quad \text{(B-17)}$$

where  $A$  and  $B$  are integration constants. Using (B-15), (B-16) and (B-17), Eq (B-14) can be written

$$0 = \frac{c^2 B^2}{\left(1 - \frac{F}{2r}\right)} - \left(1 + \frac{F}{2r}\right) \left(\frac{dr}{dq}\right)^2 - \frac{A^2}{r^2} \quad \text{(B-18)}$$

or, to first order in  $F$ ,

$$0 = c^2 B^2 - \left(\frac{dr}{dq}\right)^2 - \frac{A^2}{r^2} + \frac{A^2 F}{2r^3} \quad \text{(B-19)}$$



where, by the approximation to order F, this equation has reduced to that obtained using the exact Schwarzschild metric.

To find the trajectory as a function  $r(\phi)$  we write

$$\left(\frac{dr}{dq}\right)^2 = \left(\frac{dr}{d\phi}\right)^2 \left(\frac{d\phi}{dq}\right)^2 \quad (\text{B-20})$$

or, using (B-16),

$$\left(\frac{dr}{dq}\right)^2 = \left(\frac{dr}{d\phi}\right)^2 \frac{A^2}{r^4} \quad (\text{B-21})$$

Substituting this into (B-19) and making the change of variables,

$$u = \frac{1}{r}, \quad du = \frac{-dr}{r^2}, \quad \text{gives}$$

$$0 = c^2 B^2 - A^2 \left(\frac{du}{d\phi}\right)^2 - A^2 u^2 + \frac{A^2 F u^3}{2} \quad (\text{B-22})$$

which, by differentiating again with respect to  $\phi$ , becomes

$$0 = -2A^2 \frac{du}{d\phi} \frac{d^2u}{d\phi^2} - 2A^2 u \frac{du}{d\phi} + \frac{3A^2}{2} u^2 \frac{du}{d\phi} \quad (\text{B-23})$$

Cancelling the  $\frac{du}{d\phi}$ , which itself gives a circular orbit solution, the equation for light ray trajectories is then

$$\frac{d^2u}{d\phi^2} + u = \frac{3Fu^2}{4} \quad (\text{B-24})$$

This equation is solved by approximation where the term on the right is considered a small perturbation of order F. The zeroth order

solution, satisfying

$$\frac{d^2 u}{d\phi^2} + u = 0 \quad (\text{B-25})$$

is

$$u = u_0 \cos \phi \quad (\text{B-26})$$

a straight line, or unperturbed trajectory, in spherical coordinates, with  $r_0 = \frac{1}{u_0}$  being the impact parameter. (A constant phase term has been set to zero by aligning the axes so that  $\phi = 0$  at closest approach.) This expression is substituted into the perturbation term of (B-24) and the resulting equation, of first order in the perturbation, is solved by using a trial solution with undetermined coefficients. The result is added to (B-26) to give the full solution to first order in  $F$ , which is

$$u = \frac{1}{r} = \frac{1}{r_0} \cos \phi - \frac{F}{4r_0^2} \cos^2 \phi + \frac{F}{2r_0^2} \quad (\text{B-27})$$

The total deflection of a ray traversing the field is  $\pi$  radians minus the angle between the asymptotes to the trajectory at  $r = \infty$ . Setting  $\frac{1}{r} = \frac{1}{\infty} = 0$  in (B-27) leaves a quadratic equation for  $\cos \phi$ , which is solved to give

$$\begin{aligned} \cos \phi_\infty &= \frac{2r_0}{F} \pm \frac{1}{2} \sqrt{\frac{16r_0^2}{F^2} + 8} \\ &= \frac{2r_0}{F} \left( 1 - \sqrt{1 + \frac{F^2}{2r_0^2}} \right) \end{aligned} \quad (\text{B-28})$$

where the minus sign was chosen since  $\cos\phi$  must be less than one.

Expanding to first order in  $F$  gives

$$\cos\phi_{\infty} = \frac{-F}{2r_0} \quad (\text{B-29})$$

Since this is a very small quantity,  $\phi_{\infty}$  must be very near either  $+\frac{\pi}{2}$ , where  $\cos\phi_{\infty 1} \approx \frac{\pi}{2} - \phi_{\infty 1}$ , or  $-\frac{\pi}{2}$ , where  $\cos\phi_{\infty 2} \approx \frac{\pi}{2} + \phi_{\infty 2}$ . Thus,  $\phi_{\infty 1} = \frac{\pi}{2} + \frac{F}{2r_0}$  and  $\phi_{\infty 2} = -(\frac{\pi}{2} + \frac{F}{2r_0})$  are the angles of the asymptotes and the total deflection angle,  $\Gamma$ , is

$$\begin{aligned} \Gamma &= \pi - (\phi_{\infty 1} - \phi_{\infty 2}) \\ &= \frac{F}{r_0} = \frac{4MG}{c^2 r_0} \end{aligned} \quad (\text{B-30})$$

Now, letting  $r'$  denote the distance of closest approach to the field source, which occurs at  $\phi = 0$ ,  $\cos\phi = 1$ , we have,

$$\begin{aligned} \frac{1}{r'} &= \frac{1}{r_0} - \frac{F}{4r_0^2} + \frac{F}{2r_0^2} \\ &= \frac{1}{r_0} + \frac{F}{4r_0^2} \end{aligned} \quad (\text{B-31})$$

Solving the quadratic equation for  $r_0$  gives

$$\begin{aligned} r_0 &= \frac{r'}{2} \pm \frac{1}{2} \sqrt{r'^2 + Fr'} \\ &\approx r' \left(1 + \frac{Fr'}{4}\right) \end{aligned} \quad (\text{B-32})$$

Thus, although Eq (B-30) was derived in terms of the impact parameter, its form is the same, to first order in  $F$ , when the distance of closest

approach is used. Equation (B-30) is the standard expression for small deflection angle, and agrees with the expression determined in the main report using paraxial approximations and Huyghen's principle.

## Appendix C

### Justification of Approximations

In this appendix, the seven approximations listed in the introduction and incorporated in the main report are justified and discussed. The numerical values given in Chapter II and some of the intermediate results in the main report are used.

#### Stars and Galaxies as Point Sources

In regard to the first approximation, whereby all sources are treated as point sources, it is noted that even the closest stars are not resolvable into extended images in photographic plates. Any observable size can be attributed to a diffraction pattern, with the maximum image density being a measure of the effectively uniform intensity from the star across the telescope aperture. Stars, therefore, are indistinguishable from point sources radiating the same total power, and can be treated as such with regard to observable effects.

The extended nature of galaxies, on the other hand, is evident. However, in this case, the radiation from any differential region of the galaxy is affected by the intervening gravitational field just as would be that from a point source in the same location. It makes some uniform differential contribution to the intensity at the telescope aperture, and the brightness of the corresponding differential area of the image is changed in the same way as that of the point source. Since the ray bundles from different parts of the galaxy follow different paths through the intervening gravitational fields, the resulting

intensity changes are not uniform across the image. However, since galaxies do not have well defined boundaries, and since they are not spherical and present random aspects to the observer, the most reasonable quantity to compare in intensity distance determinations is peak intensity (corrected for orientation effects). The mean change in such peak galactic source intensities is the same as the mean change in idealized point source intensities. (It is noted, however, that due to the different magnifications of different ray bundles, one cannot really identify the intrinsically brightest point, and it is for this reason that background galaxies are not considered as sources in the second scenario in this study.) It therefore appears valid to approximate both stellar and galactic sources by point sources.

#### Stars and Galaxies as Point Masses

The point mass deflector approximation has two basic ways of breaking down. First, it may not account for actual masking of a source by the physical extent of a deflecting body. Second, the gravitational potential, which in Appendix A is shown to be the quantity of importance in the effects studied here, may not adequately be represented by that of a point source.

Considering first the case of physical masking of stars by stars, a standard solar radius is assumed for all stellar sources and deflectors. Some degree of masking will occur if a deflector center lies within the truncated cone whose surface is a standard stellar radius outside the cone defined by the observation point and the apparent circumference of the source (Figure 6). The probability of a given

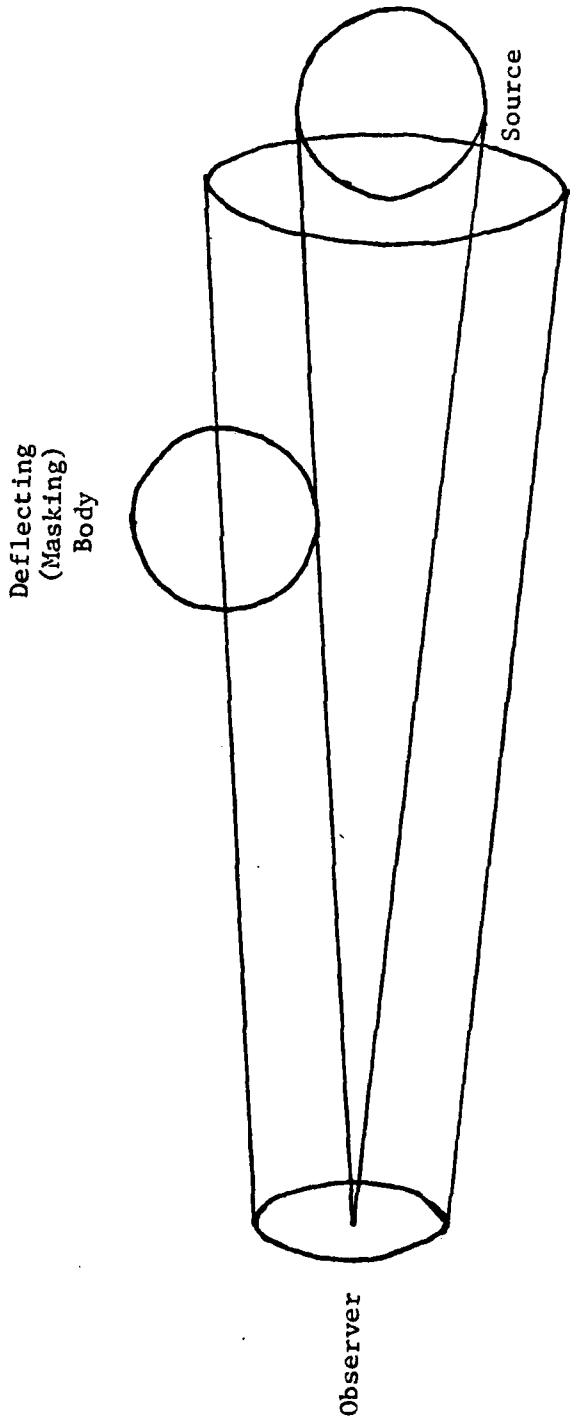


Figure 6. Volume Within Which Extended Bodies Would Physically Mask Extended Sources

source being masked to any degree is given roughly by the deflector density times the volume of that part of the outer cone lying within the intervening distribution of deflectors. The volume of the pertinent portion of cone is largest in the case of deflection by stars in another galaxy, where the cone section is essentially a cylinder of twice the standard stellar radius. Looking through a maximum 20 kpc of deflectors, its volume would be  $10^{-10} \text{ pc}^3$ . Multiplying by a star density of  $0.1 \text{ pc}^{-3}$  gives a worst case probability of any masking of a given star by an intervening star of  $10^{-11}$ . That is, of all the stars in another galaxy, viewed edge on, only perhaps one pair would be sufficiently well aligned for physical masking to occur. Within the Milky Way, using the actual conic volume reduces this probability, but even more significantly, the lower star densities and shorter ranges involved in most observations make the chances of masking much smaller still. Physical masking of stars by stars can, therefore, be safely ignored. (This, of course, does not address the possibility of masking within binary star systems).

The case of galactic deflecting masses is again rather different. In terms of masking, however, the situation is simple, since galaxies can be considered virtually transparent. They may appear opaque because the individual stars cannot be resolved, but at a wavelength that can penetrate interstellar matter, the only actual masking is that of stars in the source by stars in the deflector, and that has been shown to be negligible. Therefore, even if a source directly behind a deflecting galaxy is unresolved or undetected, its intensity contribution is not masked by the deflector. (Actually, if a deflector is indeed opaque



and hides a source behind it, then the existence of that source will be unknown and it does not really enter into the statistics.) There appears, then to be no reason why ignoring possible physical masking should invalidate the statistical results based on point mass deflectors in any of the scenarios.

The other possible source of error in the point mass approximation is in the assumption that the expression for the gravitational potential of a point mass adequately describes the fields of all real deflecting bodies. The gravitational potential at a position,  $\vec{r}$ , due to a continuous distribution of mass is given by

$$\Phi(\vec{r}) = -G \int_{\tau} \frac{\sigma(\vec{r}') d\tau'}{|\vec{r} - \vec{r}'|} \quad (C-1)$$

where  $G$  is the universal gravitational constant,  $\tau$  is the curve, surface, or volume of distributed mass, and  $\sigma$  is the associated mass density. It is evident that if  $|\vec{r}|$  is much larger than the largest dimension of  $\tau$ , then the denominator effectively becomes  $|\vec{r}| = \rho$ , which can be brought outside the integral. The remaining integral simply expresses the total mass, so that at a large distance,  $\rho$ , the potential due to a total mass,  $M$ , of any shape, approaches

$$\Phi(\rho) = \frac{-GM}{\rho} \quad (C-2)$$

which is the expression for the potential due to a point mass,  $M$ .

What is necessary, however, is to show that even at shorter ranges, depending on the scenario, expression (C-2) does not differ

greatly from the true expressions for the real deflecting masses with respect to the level of accuracy pertinent to that scenario. In the case of stellar deflectors there is no problem. They are spherically symmetric bodies with a density function of the form  $\sigma(\rho)$ . By directing the polar axis toward the field point, Eq (C-1) becomes

$$\Phi(\rho) = -G \int_0^{r_0} \int_0^\pi \int_0^{2\pi} \frac{\sigma(\rho') \rho'^2 \sin \theta' d\phi' d\theta' d\rho'}{\sqrt{\rho^2 + \rho'^2 - 2\rho\rho' \cos \theta'}} \quad (C-3)$$

and the solution in the region external to such bodies of total mass  $M$  is well known to be identical to the point mass expression (C-2). (And, as shown previously, only a negligible fraction of pertinent light rays follows trajectories which are not external to all deflecting stars.)

Galaxies, on the other hand, are not spherically symmetric, and so their potential fields are more complex than that of a point mass. The general expressions for the exact fields around these bodies are not easily calculated, even if the specific mass distribution is known, and furthermore, they are all different. Some galaxies are ellipsoids not greatly varying from spherical symmetry, some are rather disk-like spirals, some have a major bar shaped component, and some are altogether irregular. In view of the low level of accuracy involved in the galactic deflector scenario, however, it is sufficient to consider a couple of easily solvable, idealized cases in order to estimate the level of error arising from the universal application of expression (C-2).

Consider first the potential on the axis of a disk of radius  $r_0$ , which might represent an extreme spiral galaxy. By a proper orientation of axes, Eq (C-1) becomes

$$\Phi(\rho, 0, 0) = -G \int_0^{r_0} \int_0^{2\pi} \frac{\sigma(\rho', \phi') \rho' d\phi' d\rho'}{\sqrt{\rho^2 + \rho'^2}} \quad (C-4)$$

For a uniformly distributed total mass, M, the density is

$$\sigma(\rho, \phi) = \frac{M}{\pi r_0^2} \quad (C-5)$$

and the solution to (C-4) is

$$\begin{aligned} \Phi(\rho, 0, 0) &= \frac{2MG}{r_0^2} \left( \rho - \sqrt{\rho^2 + r_0^2} \right) \\ &= \frac{2MG\rho}{r_0^2} \left( 1 - \sqrt{1 + \frac{r_0^2}{\rho^2}} \right) \end{aligned} \quad (C-6)$$

which in fact approaches (C-2) in the limit  $\rho \gg r_0$ . By evaluating (C-6) and (C-2) at various points, it is evident that one need not be very far away for the two results to agree closely. At  $\rho = 2r_0$ , Eq (C-2) gives a value which is off by 6 percent. At  $\rho = 3r_0$ , the error is down to 2.5 percent, and at  $\rho = 10r_0$ , it is only 0.25 percent.

Another, probably "worst case," idealized galaxy is one composed of a bar of no thickness, length  $2r_0$ , and a uniform, linear distribution of total mass, M, given by  $M/2r_0$ , as might represent the limiting configuration of a barred galaxy. For field points on the axis defined by the bar, expression (C-1) becomes

$$\begin{aligned}\Phi(\rho, 0, 0) &= -G \int_{-r_0}^{r_0} \frac{\sigma(\rho') d\rho'}{\rho - \rho'} \\ &= \frac{-MG}{2r_0} \int_{-r_0}^{r_0} \frac{d\rho'}{\rho - \rho'}\end{aligned}\tag{C-7}$$

The solution,

$$\begin{aligned}\Phi(\rho, 0, 0) &= \frac{MG}{2r_0} \ln \left( \frac{\rho - r_0}{\rho + r_0} \right) \\ &= \frac{MG}{2r_0} \ln \left( 1 - \frac{2r_0}{\rho + r_0} \right)\end{aligned}\tag{C-8}$$

again approaches (C-2) for  $\rho \gg r_0$ . In this case, the values calculated from (C-2) are off by 9 percent at  $\rho = 2r_0$ , 3.8 percent at  $\rho = 3r_0$ , and 0.33 percent at  $\rho = 10r_0$ , only slightly worse than the errors at equal distances on the axis of the disk. This means that even for rays coming  $10^9$  pc from the edge of the universe, through a uniform distribution of  $3 \times 10^{-18}$  galaxies per cubic parsec, every one of which is bar shaped with length  $2r_0 = 20$  kpc and no thickness, with its axis directed toward the ray path, there are apt to be about four deflectors whose individual contribution to the net effect from all galaxies varies by more than 9 percent from that given by expression (C-2), (i.e.,  $\rho \leq 2r_0$ ), and about 24 with an error in excess of 1 percent ( $\rho \leq 5r_0$ ).

Now in reality, most well defined intensity sources are closer than  $10^9$  pc, and all galaxies (even barred galaxies) are much more spherical than this idealized worst case, always having some thickness,

and generally having a somewhat spheroidal central core. For a given source, then, the expected number of deflecting galaxies whose potential fields are inadequately modeled by that of a point mass is much lower than these numbers suggest.

It turns out, however, that due to the rapid drop off of gravitational effects with ray/deflector separation, these few closely aligned deflectors will make the greatest contribution to the total effect so that any error in their individual contributions might indeed be evident in the total effect. The contributions from such close alignments will in fact not be correctly included in the total effect calculated in this study and it would appear that such contributions should always be individually analyzed. However, since the objective of this study is find the mean total effect, the random orientation of deflecting galaxies is expected to result in some degree of cancellation among those contributions from individual deflecting galaxies closely aligned with sources, between errors on the high side and those on the low side. Furthermore, in the case of galactic deflectors, the required level of accuracy is only to the order of magnitude. The point mass approximation is, therefore, retained in all scenarios, recognizing that for galaxies the errors may be larger but are in keeping with the level of accuracy of that scenario.

#### Plane Wave Approximation of Celestial Radiation

The inverse square distance relation, upon which the intensity distance measurement concept is based, arises from the essentially spherical wave form of celestial radiation. In this sense, then, the

actual spherical nature of waves is fundamental to this study. However, in studying the superimposed gravitational effects, if the spherical nature of waves cannot be discerned from the available data, then there can be no need for considering spherical waves rather than simple plane waves. In this case, data collection would be confined to the region within a telescope aperture, and even at short, optical wavelengths the spherical waves from the nearest star deviate from a plane wave by only about  $4 \times 10^{-10}$  wavelengths across the 100 inch radius of the largest telescope aperture. This is probably at least  $10^7$  times smaller than the tolerances in the optical surface, and under other possible conditions the deviation would be reduced even further. (In fact, using a hundredth of a wavelength tolerance, and this aperture, a point source would have to be closer than 0.01 A.U. for the deviation of its spherical waves from plane waves to exceed the surface tolerance.) It is safe to assume, then, that the distinction between plane and spherical waves cannot be made and that all telescopes viewing stars or galaxies are focused at infinity.

It might seem that in an analysis incorporating deflecting gravitational fields which extend to infinity, the spherical nature of radiation would be evident and should be taken into account. However, the only portion of these fields which actually contributes to the observed effects, and thus should be considered, is that portion penetrated by the ray bundle entering an observer's telescope. For point sources and weak fields, the cross section of this region will never be larger than approximately the size of the receiving aperture. Thus, even for nearly equidistant sources and deflectors, the plane wave

approximation is appropriate. (Extended sources do not actually, necessarily radiate true spherical waves any way, but nonetheless, the above arguments could be applied to differential radiating areas of the source.)

#### Monochromatic Waves and the Geometrical Optics Limit

Since the gravitational index of refraction given by Eq (3-8) is independent of wavelength, the analysis can be simplified by considering monochromatic waves. Furthermore, the geometrical optics limit can be assumed (i.e.,  $\lambda \rightarrow 0$ ), since all wavelengths of interest are much smaller than the scale size,  $d$ , in any astronomical scenario considered, and since in each scenario the propagation distances (after deflection) are much less than the distance at which diffraction effects become important, given by  $d^2/\lambda$ . (The scale size of the inhomogeneities in the overall gravitational field should be comparable to the mean separation between masses, and using point masses there would be no diffraction effects from the deflecting bodies themselves.)

#### Phase Screen Approximation of Gravitational Effects

As stated in the introduction, compressing all gravitational effects into the deflector plane amounts to replacing the true hyperbolic trajectories by their pairs of intersecting asymptotes (Figure 7). For rays with larger impact parameters, the curve in the hyperbola is longer, since there is a longer distance along which the larger component of the gradient of the index of refraction is orthogonal to the trajectory. It is evident, then, that the phase screen approximation is pretty good in the region in which  $|z| > kr$ , where a higher value of  $k$  defines a

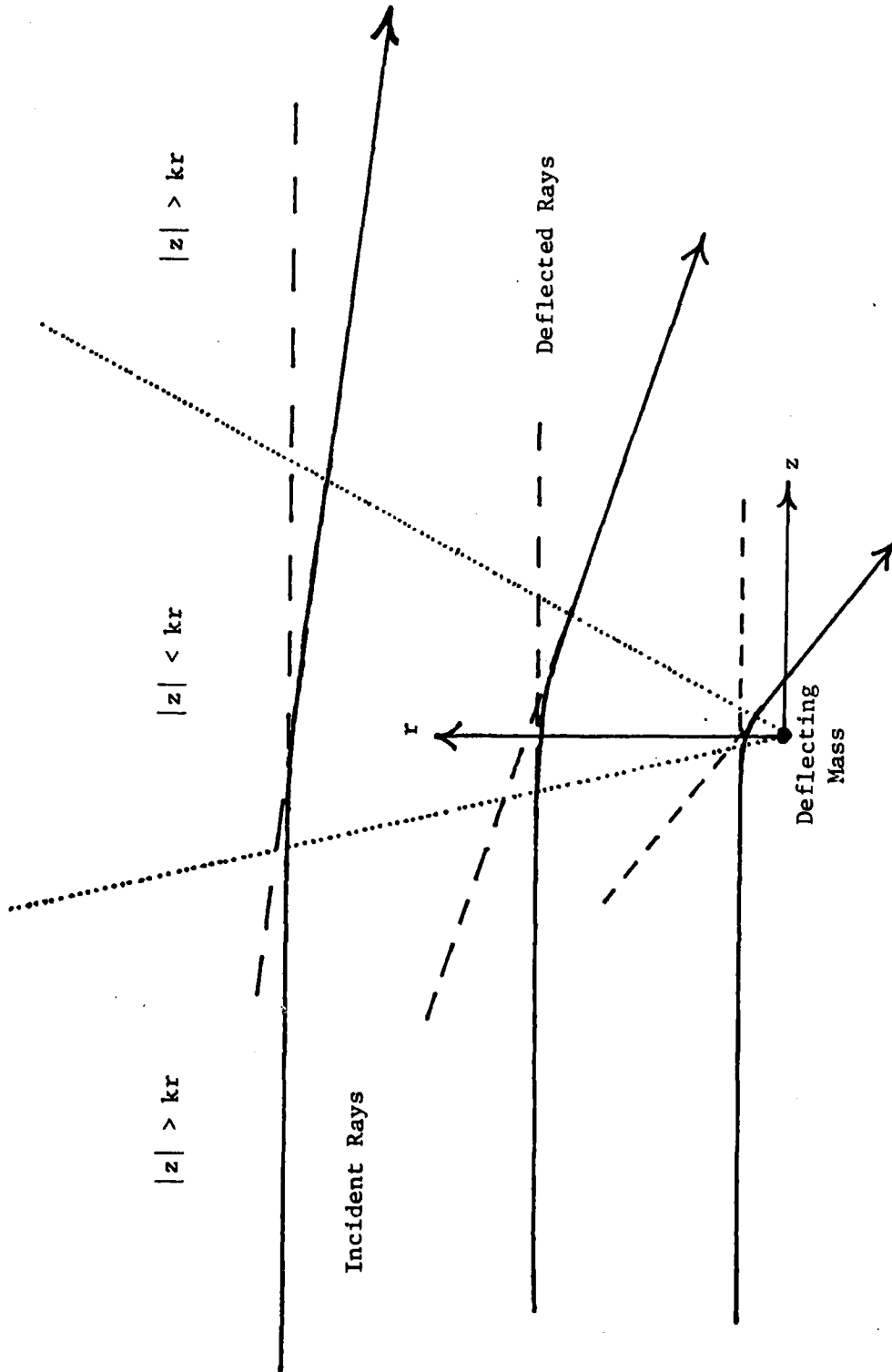


Figure 7. Rays Deflected by a Point Mass and Their Asymptotes



region of smaller maximum error, and not as good for  $|z| < kr$ . (The true relation may not be linear, but the actual form is not important in the following arguments which apply only within a certain radius.) The validity of the thin phase screen in this "far field" region is also attested to by the agreement between the total ray deflection derived using it with that resulting from the four space geodesic approach used in Appendix B.

In determining the total effect due to all deflectors, it may be that for some, the condition  $z > kr$  does not hold at the observer. (The absolute value signs have been dropped because deflectors downstream of the observer have not been considered in this study since as a result of the phase screen approximation they can have no effect.) Thus, in view of the objectives of this study, it must be shown that individual effects associated with the condition  $z < kr$  are too rare and/or too small to have any impact on the total effect.

Expression (5-3) shows that the effects of individual deflecting masses on the intensity decrease with the fourth power of their distance from the line of sight to the source, and the statistical results of Chapter VI reflect this, in that the significant contributions to the mean total effect are seen to be from those deflectors within some cylinder around the line of sight. Since the radius of this "large effect" cylinder is very small relative to its length, the region within which a deflector might lie such that it would both be within the cylinder and satisfy  $kr > z$  is very small compared to the total cylinder volume. Thus, the probable number of deflectors in that region is small. Also, from this study it appears that measurable intensity changes under

weak field conditions result from small differential ray deflections being propagated over large distances. Thus, since the above region of deflectors would necessarily be adjacent to the observer, it is assumed that the intensity changes due to each of its very few members would all be very small. Therefore, the phase screen approximations is assumed valid for all significant contributions to the total gravitational intensity change.

#### Weak Field Approximation

In the real world of extended masses, the condition for a weak gravitational field, expression (1-1), can be assumed to be met everywhere in free space except in the vicinity of black holes and perhaps neutron stars. In the universe of point masses treated in this study, on the other hand, every mass is surrounded by a region of free space of radius  $6 \times 10^{-8}$  A.U. for stars and  $10^{-2}$  pc for galaxies, in which condition (1) does not hold, and through which ray trajectories might pass. However, the numbers of idealized point stars likely to be found within  $6 \times 10^{-8}$  A.U., and idealized point galaxies within  $10^{-2}$  pc of the line of sight to an appropriate source are both negligible, since they are much smaller than the probable numbers, which were themselves negligible, calculated in the point mass discussion for stars or galaxies likely to cause physical masking. Therefore, the weak field assumption should result in no errors.

#### Paraxial Approximations

The term paraxial is used here in identifying three similar approximations introduced in this study. In the first it is assumed

that the phase perturbations to the incident waves are small enough that in some places the deflected rays can be adequately approximated by undeflected rays. A specific example is the treatment of  $r$  as a constant when integrating along deflected ray paths. This is valid if lateral displacement of rays over the propagation distance is small relative to the impact parameter. This lateral displacement, at a position downstream of the deflector, is given by

$$\begin{aligned} \text{L.D.}(r, z) &= z |\Gamma(r, z)| \\ &= \frac{2zF}{r \left[ 1 + \sqrt{1 + \frac{4Fz}{r^2}} \right]} \end{aligned} \quad (\text{C-9})$$

where expression (4-29) has been used for  $\Gamma$ , the ray deflection. The above condition can then be expressed as

$$r \gg \frac{2zF}{r \left[ 1 + \sqrt{1 + \frac{4zF}{r^2}} \right]} \quad (\text{C-10})$$

or

$$r^2 \gg \frac{2zF}{1 + \sqrt{1 + \frac{4Fz}{r^2}}} \quad (\text{C-11})$$

which can self-consistently be approximated by

$$r^2 \gg \sqrt{Fz} \quad (\text{C-12})$$

This condition is the same as that given for the intensity approximation made in Chapter V. Thus, it is regarded as a second paraxial approximation. The detailed discussion of that section therefore covers the

accuracy and validity of the paraxial approximations in both these cases.

The third paraxial approximation is the assumption that the ray paths through a distribution of deflecting masses are essentially unchanged relative to those deflector locations when other deflecting masses are added. Assuming that deflectors are located in random locations around the ray path, this will be true if the maximum lateral ray displacement within the distribution of deflectors is very small compared to the mean separation between deflectors. That this is true can be shown either by multiplying the maximum (grazing) ray deflection angles around real bodies by the maximum dimension of the distribution of deflectors (though this does not really fit into an analysis of point masses), or by calculating the maximum displacement caused by deflectors obeying condition (5-4), (which is appropriate for this study but gives only statistical support).

Using a solar radius impact parameter, the maximum deflection by a standard mass star, (i.e.,  $1.5M_{\odot}$ ), is calculated from Eq (4-25) to be  $1.3 \times 10^{-5}$  radians. Over a maximum galactic dimension of 20 kpc, this gives a displacement of .26 pc, somewhat less than the mean stellar separation distance. The grazing deflection of rays by galaxies as a whole, using  $r = 10$  kpc and  $F_g = 10^{-2}$  pc, is  $10^{-6}$  radians. The lateral displacement after  $4 \times 10^9$  pc is then 4000 pc, which is about a hundred times smaller than the mean galactic separation, easily satisfying the conditions of the approximation.

Considering only those deflectors satisfying condition (5-4), which according to Chapter V are essentially the only deflectors which

need to be considered, the maximum lateral displacement at a distance  $z$  downstream is maximized subject to condition (5-4) on its bounding paraboloid given by (5). That is

$$\begin{aligned}
 L.D._{max}(z) &= (z \Gamma)_{max} \\
 &= z \frac{F}{\sqrt{WFz}} \\
 &= \sqrt{\frac{Fz}{W}}
 \end{aligned}
 \tag{C-13}$$

with the overall maximum displacement occurring at the largest available value of  $z$ . The maximum lateral displacement by stellar deflectors, across the 20 kpc maximum galactic dimension is then  $3 \times 10^{-5}$  pc or 6 A.U. The distribution of galaxies covers the entire observable universe, so the maximum lateral displacement across its radius is 9000 pc. Keeping in mind that these are all "worst case" numbers, the third paraxial approximation is then also validated using either approach for all scenarios.

It might be noted that none of these paraxial approximation was justified solely by the fact that the maximum deflection angle itself was "small". Nevertheless, the accuracy and validity of each has been established.

VITA

George Edward Cipperly was born on 7 January 1954 in Rochester, New York. He was valedictorian of the class of 1972 at Tamarac High School in Troy, New York, and received a Bachelor of Science degree in engineering physics from Cornell University in May 1976. While at Cornell he was inducted into Tau Beta Pi and participated in the ROTC program. After being commissioned in the USAF he served as a test engineer with the 3246 Test Wing at Eglin AFB, Florida. There he directed testing of television and infrared guided weapon systems, imaging infrared sensors, and data link control systems. In June 1981 he entered the Master of Science in engineering physics degree program of the School of Engineering, Air Force Institute of Technology.

Permanent address: 15 Moonlawn Road  
Troy, New York 12180

UNCLASSIFIED

SECURITY CLASSIFICATION OF THIS PAGE (When Data Entered)

REPORT DOCUMENTATION PAGE		READ INSTRUCTIONS BEFORE COMPLETING FORM
1. REPORT NUMBER AFIT/GEP/PH/82D-4	2. GOVT ACCESSION NO. 15 1 2	3. RECIPIENT'S CATALOG NUMBER
4. TITLE (and Subtitle) THE NET EFFECT OF MANY GRAVITATIONAL FIELDS ON THE INTENSITY OF CLESTIAL LIGHT SOURCES		5. TYPE OF REPORT & PERIOD COVERED MS Thesis
		6. PERFORMING ORG. REPORT NUMBER
7. AUTHOR(s) George E. Cipperly, Captain, USAF		8. CONTRACT OR GRANT NUMBER(s)
9. PERFORMING ORGANIZATION NAME AND ADDRESS Air Force Institute of Technology Wright-Patterson AFB, Ohio 45433		10. PROGRAM ELEMENT, PROJECT, TASK AREA & WORK UNIT NUMBERS
11. CONTROLLING OFFICE NAME AND ADDRESS		12. REPORT DATE December 1982
		13. NUMBER OF PAGES 121
14. MONITORING AGENCY NAME & ADDRESS (if different from Controlling Office)		15. SECURITY CLASS. (of this report)  UNCLASSIFIED
		15a. DECLASSIFICATION/DOWNGRADING SCHEDULE
16. DISTRIBUTION STATEMENT (of this Report)  Approved for public release; distribution unlimited		
17. DISTRIBUTION STATEMENT (of the abstract entered in Block 20, if different from Report)		
18. SUPPLEMENTARY NOTES  Approved for public release: IAW AFR 190-17. <i>E. E. Wolaver</i> E. E. WOLAVER Dean for Research and Professional Development Air Force Institute of Technology (ATC) Wright-Patterson AFB OH 45433  7 APR 1983		
19. KEY WORDS (Continue on reverse side if necessary and identify by block number)  Gravitational Lens General Relativity Astrophysics		
20. ABSTRACT (Continue on reverse side if necessary and identify by block number)  This analysis shows that the mean total intensity change in celestial light sources due to the combined gravitational fields of all celestial bodies has a negligible impact on the accuracy of intensity distance measurements at any range. In the case of galactic distance measurements, however, the typical intensity changes are large enough that time variations might be observable.		

DD FORM 1 JAN 73 1473

EDITION OF 1 NOV 65 IS OBSOLETE

UNCLASSIFIED

SECURITY CLASSIFICATION OF THIS PAGE (When Data Entered)

**END**

**FILMED**

**6-83**

**DTIC**